8-2016

Applications of the homotopy analysis method to optimal control problems

Shubham Singh
Purdue University

Graduate School Form
30 Updated 12/26/2015

PURDUE UNIVERSITY
GRADUATE SCHOOL
Thesis/Dissertation Acceptance

This is to certify that the thesis/dissertation prepared

By SHUBHAM SINGH

Entitled
APPLICATIONS OF THE HOMOTOPY ANALYSIS METHOD TO OPTIMAL CONTROL PROBLEMS

For the degree of Master of Science in Aeronautics and Astronautics

Is approved by the final examining committee:

Michael J. Grant
Chair

James M. Longuski

William A. Crossley

To the best of my knowledge and as understood by the student in the Thesis/Dissertation Agreement, Publication Delay, and Certification Disclaimer (Graduate School Form 32), this thesis/dissertation adheres to the provisions of Purdue University's "Policy of Integrity in Research" and the use of copyright material.

Approved by Major Professor(s): Michael J. Grant

Approved by: Weinong Wayne Chen 8/5/2016

Head of the Departmental Graduate Program Date

APPLICATIONS OF THE HOMOTOPY ANALYSIS METHOD TO OPTIMAL CONTROL PROBLEMS

A Thesis

Submitted to the Faculty

of

Purdue University

by

Shubham Singh

In Partial Fulfillment of the

Requirements for the Degree

of

Master of Science in Aeronautics and Astronautics

August 2016

Purdue University

West Lafayette, Indiana

Dedicated to Dr. A.P.J. Abdul Kalam

ACKNOWLEDGMENTS

First of all, I would like to thank my family for the constant encouragement to pursue my dreams. Their constant support throughout the journey has kept me focused and inspired to perform well in graduate school.

I am highly thankful to Professor Michael Grant for introducing me to the area of hypersonic mission design, encouraging me to work hard and helping me to develop the required skills needed to work in this area. His extensive course on Hypersonic Performance and Design was the foundation of my research career at Purdue. I would also like to express my gratitude to Professor William Crossley and Professor James Longuski for teaching the courses which helped me to understand the basics of optimization theory. I am thankful to them for serving on my committee and reviewing my thesis. I also offer my gratitude to Professor Gregory Blaisdell for his essential advice at the beginning of my graduate school life. His caring nature and availability to help students in planning their graduate school studies is valuable.

I would specifically like to thank Kshitij Mall for offering me advice throughout the hardships of graduate school. It is because of him that I have been able to handle hard situations. I am indebted to Max Fagin for being a very helpful friend and teammate during the graduate school. I am also grateful to Zhenbo Wang, Thomas Antony, Harish Saranathan and everyone in my research group to assist me from time to time.

Finally, I would like to acknowledge the Department of Physics, Purdue University and Professor Andrzej Lewicki to provide Teaching Assistantship which helped me to support my graduate studies partially.

TABLE OF CONTENTS

Page

LIST OF TABLES

LIST OF FIGURES

SYMBOLS

J	Cost functional
$\mathscr{L}$	Path cost
η	Terminal cost
$\boldsymbol{\nu}$	Lagrange multiplier of adjoined constraint
$\boldsymbol{x}$	State vector
$\boldsymbol{\lambda}$	Co-state vector
$\boldsymbol{u}$	Control vector
$\mathscr{H}$	Hamiltonian
U	Set of admissible controls
$\boldsymbol{\Phi}$	Initial constraint vector
$\boldsymbol{\Psi}$	Terminal constraint vector
n	Order of a general non-linear ODE
N	General non-linear ODE
t	Time variable
r	Spatial variable
a	Positive real number
k	Positive integer
B	Linear operator
q	Embedding parameter
ϕ	Homotopy-Maclaurin series solution for a state u
ψ	Homotopy-Maclaurin series solution for a state w
x_0	HAM initial guess for the state x
L	Linear operator
c_o	Convergence control parameter
H_a	Auxiliary function

m	Order of the deformation derivative
δ_k	k^{th} order of the homotopy derivative operator
f	General smooth function in a single variable
g	General smooth function in two variables and gravitational constant, m/s^2
K_1	Highest order of derivative of the general governing equation
K_2	Positive integer
β_i	Parameter for unknown initial boundary conditions
t_f	Unknown final time value
θ	Steering angle for Zermelo's problem, deg
α	Steering angle for 2D ascent problem, deg
F	Vehicle thrust force, N
y	State variable
h	Altitude, km
R	Horizontal range, km
v_x	Horizontal velocity, km/s
v_y	Vertical velocity, km/s

ABBREVIATIONS

GPOPS	General Purpose Optimal Control Software
NLP	Non Linear Programming
BVP	Boundary Value Problem
ODE	Ordinary Differential Equation
PDE	Partial Differential Equation
HAM	Homotopy Analysis Method
HPM	Homotopy Perturbation Method
TPBVP	Two Point Boundary Value Problem
OCP	Optimal Control Problem

ABSTRACT

Singh, Shubham, MS, Purdue University, August 2016. Applications of the Homotopy Analysis Method to Optimal Control Problems. Major Professor: Michael J. Grant.

Traditionally, trajectory optimization for aerospace applications has been performed using either direct or indirect methods. Indirect methods produce highly accurate solutions but suffer from a small convergence region, requiring initial guesses close to the optimal solution. In past two decades, a new series of analytical approximation methods have been used for solving systems of differential equations and boundary value problems.

The Homotopy Analysis Method (HAM) is one such method which has been used to solve typical boundary value problems in finance, science, and engineering. In this investigation, a methodology is created to solve indirect trajectory optimization problems using the Homotopy Analysis Method. Use of the auxiliary convergence control parameter to widen the convergence region and increase the rate of convergence have been demonstrated on multiple optimal control problems. The guaranteed convergence and the ease of selecting the initial guess for trajectory optimization problems makes the method of high significance. It has been demonstrated that initial guesses for the optimal control problem can be generated using a simple approach based on only the initial boundary conditions. The approach has been demonstrated on the Zermelo's problem and two cases of a 2D ascent problem. It has been established that for free final-time boundary value problems, finding the convergence region is much harder as compared to fixed final-time cases. To validate the approach, results are compared with those obtained using the MATLAB's *bvp4c* function. A number of new challenges are discovered and listed during the process.

1. INTRODUCTION

Conventionally, trajectory optimization for conceptual hypersonic mission design applications has been performed using the direct [1–3] and the indirect methods [4]. Continuous progress has been made over the years which led to more complex and computationally expensive solvers. However, for most of the current trajectory optimization methods, proving guaranteed convergence of the optimal solution is a very challenging task.

Direct methods are based on discretizing the non-linear optimal control problem parameterized by the nodes containing the state and control information. Parametric optimization techniques are then used to optimize the nodes which satisfy a set of initial, terminal and path constraints. Current state-of-the-art solvers used in government and industry are contained in programs like DIDO [5] and GPOPS [6], implement pseudo-spectral [7] and collocation [8] methods which result in a computationally intensive Non Linear Programming (NLP) problem. Solvers like SNOPT [9] are used to handle these large optimization problems.

Indirect methods, on the other hand, are based on Calculus of Variations [10] and Pontryagin's Minimum Principle [11]. The optimal control problem is formulated as a boundary value problem which can be solved using either indirect shooting [12] or collocation methods. Since indirect methods use the necessary conditions of optimality, the trajectories produced are much more accurate as compared to direct methods, which makes them valuable in the aerospace community. Study in Ref. [13] found out that, solving optimal control problems using the direct methods resulted in errors of upto 1% in the minimum functional value. Sometimes, the discretization of a trajectory leads to "pseudominima", where the solution is far away from the true solution which satisfies the necessary conditions of optimality [14]. For hypersonic vehicles traveling with speeds as high as Mach 5-8, on-board guidance algorithms

are required to control the vehicle. Minimum human interaction is intended, which creates a need of highly reliable guidance algorithms. Since, the convergence properties of a trajectory optimization method is critical for onboard applications, indirect methods are often discarded due to their poor convergence properties. As an indirect trajectory optimization problem concludes in solving a boundary value problem, a search for methods to solve non-linear boundary value problems was done. Analytical approximation methods are a technique to solve non-linear ordinary and partial differential equations. They have been applied to problems arising in science and engineering in the past two decades, but their application to trajectory optimization problems has not been thoroughly studied. These methods are reported to have good convergence properties and produce high quality approximate solutions [15]. Some popular analytical approximate methods developed to solve non-linear ordinary differential equations (ODEs), partial differential equations (PDEs) and Boundary Value problems (BVPs) include the following

1. Variational Iteration Method [16]
2. Adomian Decomposition Method [17]
3. Lyapunov's Artificial Small Parameter Method [18]
4. δ - Expansion Method [19]
5. Perturbation Methods [20]
6. Homotopy Analysis Method (HAM) [21]

The Homotopy Analysis Method in particular has gained popularity to solve boundary value problems arising in science, finance and engineering after it was proposed by Dr. Shijun Liao in 1992 [22]. It has been proven that HAM logically contains the methods 2-5 listed above [23, 24]. Perturbation methods are strongly dependent on small physical parameters, called perturbation quantities, which are present in the system of equations. Unfortunately, not every nonlinear problem has perturbation

quantities, and thus, it is not guaranteed that the perturbation method will converge to a solution. The Homotopy Perturbation Method (HPM) [25] is an example of a popular perturbation method used to solve BVPs. Since Homotopy Analysis Method is independent of any small or large parameters, guarantees convergence [26], and provides great flexibility in the choice of initial guess, this investigation has assessed its use to solve indirect trajectory optimization problems. By application on several optimal control problems, it has been demonstrated that trivial initial guesses based only on the initial boundary conditions can be used to obtain converged solutions. An initial framework has been developed to apply the HAM approach on aerospace applications. A basic review of indirect trajectory optimization is given in the Chapter 2. The application of HAM to optimal control problems is explained in Chapter 3. Zermelo's problem and two cases based on a 2D Ascent problem are solved using the HAM approach in Chapter 4. It has been demonstrated that using trivial initial guesses, HAM is able to successfully solve optimal control problems.

2. INDIRECT TRAJECTORY OPTIMIZATION

Indirect methods for trajectory optimization are called as such due the fact that the resulting optimal control problem (OCP) is tackled indirectly by first using Calculus of Variations and further solving a boundary value problem [27]. However, the aerospace engineering community is well aware of the challenges associated with indirect methods, the majority of which can be summarized as follows:

1. Small convergence domain due to local convergence properties and numerical instabilities. Sometimes, the solution is hypersensitive to the initial guess due to the symplectic nature of the Hamiltonian system. This requires an initial guess close to the optimal solution.

2. Solving the necessary conditions of optimality requires a deep understanding of the underlying physics of the problem and hence, is a labor intensive process.

2.1 Calculus of Variations

In 1696, John Bernoulli formulated and solved the famous Brachistochrone problem. He posed the problem as:
"Given two points A and B in a vertical plane acted only by the gravity, what is the curve traced by a frictionless mass which starts at the point A and reaches point B in the minimum time."
A number of mathematicians including, Sir Isaac Newton, Jacob Bernoulli, Leibnitz and de L'Hôpital solved the problem and submitted their solutions. This led to the discovery of a whole new field of mathematics known as the Calculus of Variations, which has lot of important applications. Calculus of Variations is used to find the extrema of functionals, defined as mappings from a set of functions to real numbers.

Trajectory optimization problems are often posed as optimal control problems, where the inputs to the systems are functions, and a particular input function is desired which minimizes the required performance index. For simplicity, the discussion in this study is limited to unconstrained trajectory optimization problems only. A typical unconstrained trajectory optimization problem to minimize a continuous time cost functional, J, with path cost, $\mathscr{L}$, and terminal cost, η, is given in Eq. (2.1).

$$\begin{aligned} \text{Minimize } J = \eta(t_f, \boldsymbol{x}_f) + \int_{t_o}^{tf} \mathscr{L}(t, \boldsymbol{x}, \boldsymbol{u}) dt \\ \dot{\boldsymbol{x}} = \boldsymbol{f}(t, \boldsymbol{x}, \boldsymbol{u}) \\ \boldsymbol{\Phi}(t_0, \boldsymbol{x}_0) = 0 \\ \boldsymbol{\Psi}(t_f, \boldsymbol{x}_f) = 0 \\ \boldsymbol{u} \in U \end{aligned} \tag{2.1}$$

where $\boldsymbol{x}$ is the state vector, $\boldsymbol{f}$ is the set of process or system equations, $\boldsymbol{u}$ is the control vector, U is the set of admissible controls, $\boldsymbol{\Phi}$ and $\boldsymbol{\Psi}$ are the sets of initial and terminal boundary conditions on the state vector respectively. The Euler-Lagrange theorem defines a Hamiltonian, $\mathscr{H}$, in Eq. (2.2), and $\boldsymbol{\lambda}$ is the set of adjoint or costate variables. $\boldsymbol{\nu}_0$ and $\boldsymbol{\nu}_f$ are the sets of unknown parameters used to adjoin the boundary conditions to the cost functional. The first-order necessary conditions of optimality given by Eq. (2.3-2.7) results in a Two-Point-Boundary-Value-Problem (TPBVP).

$$\mathscr{H} \equiv \mathscr{L} + \boldsymbol{\lambda}^T \boldsymbol{f} \tag{2.2}$$

$$\frac{\partial \mathscr{H}}{\partial \boldsymbol{u}} = 0 \tag{2.3}$$

$$\dot{\boldsymbol{\lambda}}^T = -\frac{\partial \mathscr{H}}{\partial \boldsymbol{x}} \tag{2.4}$$

$$\boldsymbol{\lambda}^T(t_0) = -\boldsymbol{\nu}_0^T \frac{\partial \boldsymbol{\Phi}}{\partial \boldsymbol{x}(t_0)} \tag{2.5}$$

$$\boldsymbol{\lambda}^T(t_f) = \frac{\partial \boldsymbol{\Phi}}{\partial \boldsymbol{x}(t_f)} + \boldsymbol{\nu}_f^T \frac{\partial \boldsymbol{\Psi}}{\partial \boldsymbol{x}(t_f)} \tag{2.6}$$

$$\left(\mathscr{H} + \frac{\partial \boldsymbol{\Phi}}{\partial t} + \boldsymbol{\nu}_f^T \frac{\partial \boldsymbol{\Psi}}{\partial t} \right) \Bigg|_{t=t_f} = 0 \tag{2.7}$$

Eq. (2.7) is valid only if t_f is free to optimize, and is known as the Transversality Condition. Pontryagin's Minimum Principle is used to determine the control law at each point in time. It states that, for a local optimum, the Hamiltonian should lie at the extremum over the set of admissible controls. Eq. (2.8) gives the formal result for Pontryagin's Minimum Principle. This principle also results in the Legendre-Clebsch Necessary Condition given by Eq. (2.9) which states that the matrix $\mathscr{H}_{uu}$ must be positive semi-definite.

$$\mathscr{H}(\boldsymbol{x}^*, \boldsymbol{\lambda}^*, \boldsymbol{u}^*, t) \leq \mathscr{H}(\boldsymbol{x}^*, \boldsymbol{\lambda}^*, \boldsymbol{u}, t) \tag{2.8}$$

where $\boldsymbol{x}^*$, $\boldsymbol{\lambda}^*$ and $\boldsymbol{u}^*$ are the optimal states, costates, and control law.

$$\mathscr{H}_{\boldsymbol{u}} = 0, \; \mathscr{H}_{\boldsymbol{uu}} \geq 0 \tag{2.9}$$

where $\mathscr{H}$ is second-order differentiable in $\boldsymbol{u}$.

2.2 Methods for Indirect Trajectory Optimization

The TPBVP formulated in the last section can be root-solved to give trajectories which guarantee the necessary conditions of optimality. The most popular methods used for indirect trajectory optimization are given as follows:

1. Shooting Methods

   In the single shooting method, the Hamiltonian system is propagated in the forward or the backward direction using the Runge-Kutta 4^{th} order or similar integration scheme after guessing the unknown boundary conditions at one end of the time interval. The conditions obtained at the other end are compared with the required quantities. If the difference between the two sets of conditions is

more than a specified tolerance, the unknown initial conditions are adjusted and the process is repeated. Single shooting method generally suffers from sensitivity of variables. Small changes early in the trajectory can be propagated till the end. The Multiple Shooting Method [28] has been developed to overcome this numerical difficulty of the single shooting method. The time interval of interest, $[t_0,t_f]$ is divided into subintervals and the shooting method is used over each interval. An additional condition for continuity is also enforced on the ends of the subintervals, which increases the size of the problem. Due to the issues caused by the sensitivity of problems, very good initial guess is required for guaranteed convergence.

2. Collocation Method

   In a typical Collocation Method, the state and costate variables are represented as piecewise cubic polynomials, and the time interval is divided into a mesh. The differential equations are discretized along the time mesh. The discretized system and boundary conditions result in a system of nonlinear algebraic equations. It leads to a root-finding problem, where the unknown coefficients for the piecewise polynomials are calculated using an appropriate root-finding technique like the Newton's iteration method. A very popular solver based on this method is MATLAB's *bvp4c* [29] function. It is well known that if the nonlinearity in the problem is high, *bvp4c* requires an initial guess close to the optimal solution for convergence.

   In general, indirect methods suffer from a very common issue of, "Singular Jacobian". It is usually caused by a trajectory optimization problem with no solution, ill-conditioning of the non-linear problem and invertibility of the Jacobian matrix. To deal with the above mentioned issues, a number of studies have been conducted to build good initial guesses and improve the convergence properties of indirect methods.

2.3 Initial Guess for Indirect Methods

One of the major issues of indirect methods is the construction of an initial guess for the adjoint variables, which in most cases are non-physical quantities. Homotopy continuation techniques [30], in which a family of problems is constructed by using an "embedding parameter" are currently employed to generate good initial guesses. On progressing the value of the embedding parameter, a homotopy path can be obtained to solve a difficult problem. The solution to a simpler problem can be used as initial guess for the next problem in the homotopy chain of problems. The step size for the embedding parameter is obtained generally by trial and error. In Ref. [31], a modified approach of homotopy continuation is used to solve for the optimal descent of the second stage of a space shuttle subjective to reradiative constraints. They selected the maximum permitted skin temperature as the homotopy embedding parameter and employed the multiple shooting algorithm to solve the TPBVP. In Ref. [4], a simple continuation is used to solve highly constrained trajectory optimization problems. Instead of building an initial guess for the full trajectory, they propagated the states and costates in the reverse direction for 1 second which resulted in smooth trajectories for that short interval of time. The short unconstrained trajectory was then used to seed the problems of interest through a simple continuation process. In Ref. [32], a self-contained method was developed based on the continuation approach to solve the shuttle re-entry problem. The approach was based on constructing an auxiliary OCP in which the costates are zero and then applying a continuation method to reach the original OCP. One of the continuation parameters, $c_1 \in [0, 1]$, is used on the both the path and the terminal cost functions. A second continuation parameter, $c_2 \in [0, 1]$, is used on the terminal boundary conditions. First, c_1 is increased from 0 to 1 to obtain the original cost functional following which c_2 is increased to 1 to enforce the boundary conditions. In Ref. [33], an approach based on the homotopy continuation method for solving an orbit transfer problem was developed. A set of optimal control

problems based on an embedding parameter, λ, was defined to connect the problem of minimum energy at $\lambda = 0$ to on of minimum fuel consumption for $\lambda = 1$.

Research has also attempted to obtain initial guesses using solutions from direct methods [13,34,35], which resulted in the development of so-called "hybrid methods". The most common approach is to estimate the costates using Legendre Pseudospectral methods. The authors of Ref. [13] employed a hybrid method of direct collocation and indirect multiple shooting method. Their objective was to combine good convergence properties of direct collocation methods with the accuracy of the multiple shooting method. Initial values for the adjoint variables was needed in advance. They discovered that the grid points of the direct method yield a good choice for the positions of the multiple shooting nodes. The approach was successfully demonstrated on a minimum heat load descent trajectory of the Apollo capsule. They started with the direct collocation method to generate an initial trajectory at nine equidistant grid points. Using the direct solution, they generated the positions of the multiple shooting nodes and the values of the state and costate variables at those nodes. The final converged solution was obtained by using the multiple shooting method. The Collocation And Multiple Shooting Trajectory Optimization Software (CAMTOS) [35] was also developed to leverage the advantages of both classes of methods. The method was also demonstrated for an Ariane 5 dual payload mission design. The author modeled the lower stage of the mission, which includes all the atmospheric effects, using the direct multiple shooting method and an indirect method based on a modified Newton method for the upper stage burns.

Sometimes, using pseudospectral methods to generate initial guess for path constrained problems result in abnormalities in the trajectories. If the node spacing is large, then the dynamics can be ignored in large parts of the trajectories. This might lead to an improper initial guess for the indirect methods.

Owing to the poor convergence and numerical instabilities of the shooting and the collocation-based indirect methods, there is a need to explore a different class of methods for trajectory optimization. Analytical approximation methods provide an

immense freedom in selection of the initial guess and provide a means to control the rate and region of convergence. Therefore, they can be a revolutionary approach to solve nonlinear trajectory optimization problems.

3. HOMOTOPY ANALYSIS METHOD THEORY

The Homotopy Analysis Method is an analytic approximation method based on the concept of homotopy in topology to solve non-linear differential equations and BVPs. It is independent of any artificial parameter, provides great flexibility in the choice of initial guess, and gives designers the luxury of controlling the convergence region of the problem. Shijun Liao and other authors have demonstrated the validity of the Homotopy Analysis Method by solving boundary value problems and ordinary differential equations resulting from select highly non-linear problems.

To demonstrate the validity of HAM, Shijun Liao solved a series of problems arising in the area of boundary layer and Blasius flows over flat plates and compared the analytical HAM solutions with numerical results from other studies [36–42]. Most of the problems resulted in second and third order boundary value problems with governing equations in the form of partial differential equations. Since, the problems he solved were highly sensitive to small differences in the initial conditions, in one study [36], he found a new branch of solutions which the numerical methods failed to obtain. In another study, he was able to find a fully analytic solution of Blasius' viscous flow for the first time [38] and an analytic solution of the temperature distribution of the viscous flow past a semi-infinite flat plat [39]. He also showed how the convergence region of the power series solution can be increased and, that Blasius' power series solution is a special case of the solution obtained by HAM. Dr. Liao also solved the full non-linear Navier-Stokes equation for the incompressible steady-state laminar flow past a sphere in a uniform stream [42]. The 10^{th} order HAM drag solution agrees well with the experimental data for Reynolds number less than 30.

Abbasbandy used the HAM approach to solve nonlinear boundary value problems with multiple solutions [43–46]. In one of the studies, he was able to obtain dual solutions of a nonlinear reaction diffusion model of a porous catalyst, a problem in

chemical kinetics by solving a second order boundary value problem. He discovered that multiple solutions can be obtained through HAM by using the same initial guess and controlling the convergence region of the problem [43]. Abbasbandy [44] also used the HAM approach to solve a generalized Hirota-Satsuma coupled KdV system of equations which is used to represent the interaction of two long waves with different dispersion relations. He compared the results with other analytic approximation methods and obtained improved convergence properties of the series solutions by using the HAM convergence control parameter. In another study, Abbasbandy [45] demonstrated the use of HAM to solve the nonlinear equations of the heat radiation and conduction equations of a cooling fin, which is generally used to transfer large amounts of heat from surfaces. He validated the approach by comparing the results with the exact solution and with the ones obtained from the Homotopy Perturbation Method (HPM). He concluded that the HPM results are valid only for a small parameter in the governing equations and hence established the superiority of HAM over HPM for obtaining analytical series solutions.

To address the existence of multiple solutions to boundary value problems, Abbasbandy and Shivanian [46] developed the Predictor HAM (PHAM) approach to calculate multiple analytical branches of the solutions simultaneously with a single initial guess. It must be noted that the use of the convergence control parameter plays an important role in finding the multiplicity of the solutions for boundary value problems using HAM. HAM has also been applied to the projectile motion of a sphere for a quadratic resistance law. The resulting system was a first order initial value problem with two equations of motion. The HAM solution was shown to match the solution obtained from a Runge-Kutta solver [47].

HAM has also been used to solve linear and non-linear optimal control problems. Abbasbandy and Shirzadi [48] used the Homotopy Analysis Method to solve boundary value problems arising from problems in the Calculus of Variations. They demonstrated the use of HAM by solving the Euler-Lagrange equation for the Brachistochrone problem given by

$$y'' - yy'' - \frac{y'^2}{2} - \frac{1}{2} = 0 \tag{3.1}$$

subject to the boundary conditions, y(0) = 0 and y(1) = -0.5. Shateyi and Nik [49] applied the HAM approach to solve the Hamilton-Jacobi-Bellman (HJB) partial differential equation arising from a non-linear optimal control problem. The authors also solved three fixed final time nonlinear OCPs and demonstrated the use of multiple convergence control parameters to adjust the region of convergence. They defined a so-called "Averaged Squared Residual Error" of the governing equations and developed the optimal HAM (oHAM) method by minimizing it. Zahedi and Nik [50] applied the original HAM approach to solve finite time linear OCPs with quadratic performance index. Since the problems solved were linear, they compared the HAM results with the exact analytical solutions and found good agreement between the two solutions.

A hybrid method based on HAM and a spectral collocation technique called SHAM [51] is widely popular in the area of hyperchaotic systems. These systems are characterized to show extreme chaotic behaviors due to an infinitesimal change in the initial state values. Effati, Nik and Jajarmi [52] used a HAM based method called the Piecewise Spectral HAM (PSHAM) [53] to solve the hyperchaotic Chen system, the governing equations for which are given by Eq. (3.2)

$$\begin{aligned} \dot{x} &= a(y - x) + w + u_1 \\ \dot{y} &= dx - xz + cy + u_2 \\ \dot{z} &= xy - bz + u_3 \\ \dot{w} &= yz + rw + u_4 \end{aligned} \tag{3.2}$$

where state variables are given by x, y, z, w and u_1, u_2, u_3 and u_4 are the control inputs. They used *bvp4c* to solve the same problem and found a good agreement with the results obtained from PSHAM. Although, the Chen system is highly sensitive to initial guess provided, the governing equations does have a high degree of non-linearity. The authors of Ref. [54] used SHAM to develop an algorithm to solve non-linear optimal

control problems. They demonstrated the approach by constructing optimal maneuvers of a rigid asymmetric spacecraft and compared the solutions obtained with *bvp4c* function. The TPBVP solved was a fixed final-time interval problem with a very low degree of non-linearity. On comparison to the studies mentioned above, the current investigation discusses free final-time interval optimal control problems with very high non-linearity embedded in the governing equations. As a part of the contribution, new challenges related to the application of the HAM approach to optimal control problems are discovered, and methods to deal with them are suggested.

3.1 HAM Description

A basic idea of the HAM theory [23,55] for a general ordinary differential equation is given below. The discussion will be extended to solve a general boundary value problem. Due to tediousness of the approach, the technique is first demonstrated by solving a simple optimal control problem. Let one of the governing equations be given by an n^{th} order non-linear ODE

$$N[u(r,t),t] = 0, t \in [0,a] \tag{3.3}$$

subject to n linear boundary conditions,

$$B_k[r,t,u] = \gamma_k, 1 \leq k \leq n \tag{3.4}$$

where, N is the n^{th} order differential operator, B_k is a linear operator, u(t) is an unknown smooth function, t is a temporal variable, r is the spatial variable, and $a \geq 0$. For each governing equation N, using an embedding parameter q, Dr. Liao suggested to construct a zeroth-order homotopy deformation equation given by Eq. (3.5), so that the Homotopy-Maclaurin series solution for N, given by $\phi(r,t;q)$, exists and is analytic at $q = 0$. The analytic solution at $q = 0$ is defined as the initial guess and is provided by the designer.

$$(1-q)L[\phi(r,t;q)-u_0(r,t)] = c_o q H_a N(t,\phi(r,t;q)),\ c_o \neq 0 \tag{3.5}$$

In Eq. (3.5), $u_0(r,t)$ is the initial guess, L is a linear operator provided by the user, c_o is an auxiliary convergence control parameter, and H_a is a non-zero auxiliary function. For finite time interval BVPs, where $t \in [0,a]$, H_a is simply assigned as 1. Its significance is mostly identified in the BVPs with infinite time interval, i.e $t \in [0,+\infty]$, where it is used to ensure convergence. These problems are mostly characterized by exponentially decaying solutions. For $q=0$, Eq. (3.5) becomes,

$$L[\phi(r,t;q)-u_0(r,t)] = 0 \tag{3.6}$$

which is equivalent to

$$\phi(r,t;0) = u_0(r,t) \tag{3.7}$$

and at $q=1$, Eq. (3.5) reduces to,

$$N(\phi(r,t;q),t) = 0 \tag{3.8}$$

which is the solution for the original Eq. (3.3) provided

$$\phi(r,t;1) = u(r,t) \tag{3.9}$$

Thus by Eq. (3.7) and Eq. (3.9), it can be observed that as the embedding parameter, q increases from 0 to 1, $\phi(r,t;q)$ deforms continuously from $u_0(r,t)$ to $u(r,t)$, the solution to the original equation Eq. (3.3). By Taylor's theorem, the power series expansion of $\phi(r,t;q)$ in the variable q can be written as

$$\phi(r,t;q) = \phi(r,t,0) + \sum_{m=1}^{+\infty} \frac{1}{m!} \frac{\partial^m \phi(r,t;q)}{\partial q^m}\bigg|_{q=0} q^m \tag{3.10}$$

Dr. Liao defined the so called m^{th} order deformation derivative [23] as follows

$$u_m(r,t) = \frac{1}{m!} \frac{\partial^m \phi(r,t;q)}{\partial q^m}\bigg|_{q=0} \tag{3.11}$$

We can simplify the Eq. (3.10) by using Eq. (3.7) and Eq. (3.11) to obtain Eq. (3.12)

$$\phi(r,t;q) = u_0(r,t) + \sum_{m=1}^{+\infty} u_m(r,t)q^m \tag{3.12}$$

We assume that the linear operator, initial guess, the auxiliary convergence control parameter, and the auxiliary function are chosen such that the solution $\phi(r,t;q)$ of the zeroth-order deformation Eq. (3.5) exists, the m^{th} order deformation derivative given by Eq. (3.11) exists for all values of m, and the power series given by Eq. (3.12) converges at $q = 1$. Substituting $q = 1$ in Eq. (3.12) and using Eq. (3.9) , the solution series, u(t) is given as

$$u(r,t) = u_0(r,t) + \sum_{m=1}^{+\infty} u_m(r,t) \tag{3.13}$$

where the unknown $u_m(r,t)$ is obtained by the so-called m^{th} order deformation equation. Differentiating the zeroth order deformation equation (Eq. (3.5)) m times with respect to the embedding parameter q and then dividing it by $m!$, we obtain the m^{th} order deformation equation given by Eq. (3.14)

$$L[u_m(r,t) - \chi_m u_{m-1}(r,t)] = c_o H_a R_m(u_{m-1}, r, t) \tag{3.14}$$

subject to the linear boundary conditions,

$$u_m(r,0) = 0 \tag{3.15}$$

where

$$\chi_m = \begin{Bmatrix} 0, m \leq 1, \\ 1, m > 1 \end{Bmatrix} \tag{3.16}$$

and $R_m(u_{m-1}, r, t)$ is defined as

$$R_m(u_{m-1}, r, t) = \frac{1}{(m-1)!} \frac{\partial^{m-1} N[\phi(r,t;q)]}{\partial q^{m-1}}\bigg|_{q=0} \tag{3.17}$$

Substituting Eq. (3.12) and Eq. (3.17) into the m^{th} order deformation Eq. (3.14), we obtain Eq. (3.18)

$$L[u_m(r,t) - \chi_m u_{m-1}(r,t)] = c_o H_a \left(\frac{1}{(m-1)!} \frac{\partial^{m-1} N[\sum_{m=0}^{+\infty} u_m(r,t) q^m]}{\partial q^{m-1}} \right) \Bigg|_{q=0} \tag{3.18}$$

The new m^{th} order deformation equation (Eq. (3.18)) contains the same initial guess, linear operator, the auxiliary convergence control parameter and the auxiliary function as the zeroth order deformation Eq. (3.5). The $(m-1)^{th}$ order homotopy derivative operator given by Eq. (3.17) can be applied to any nonlinear operator N and results in the term u_{m-1}, as explained by the properties of the homotopy derivative operator later in the section. Hence, the right hand side of the m^{th} order deformation equation (Eq. (3.18)) is only dependent on the term u_{m-1}. For each value of m = 1,2,3,..., we obtain a deformation equation in u_{m-1}, which can be solved to obtain the term u_m. In practice, the series solution given by Eq. (3.13) is truncated to a finite number of terms. Thus, the resulting M^{th} order approximation is given as:

$$u(t) \approx u_0(r,t) + \sum_{m=1}^{M} u_m(r,t) \tag{3.19}$$

For simplicity, the m^{th} order homotopy derivative operator is denoted as δ_m in Eq. (3.20)

$$\delta_m(\phi) = \left(\frac{1}{m!} \frac{\partial^m \phi}{\partial q^m} \right) \Bigg|_{q=0} \tag{3.20}$$

3.1.1 Properties of Homotopy Derivative Operator

To deduce the right hand side of Eq. (3.18), the application of the $(m-1)^{th}$ order homotopy-derivative operator on the non-linear operator N is required. For majority of problems, the following set of properties are used (extensive proof for which are provided in HAM theory [26]). Some of the commonly used properties are given below. We begin by assuming a non-linear operator N, which depends on the two states, u and w. The Homotopy-Maclaurin series solutions for the two states are assumed as ϕ and ψ where,

$$\phi = \sum_{k=0}^{+\infty} u_k q^k \ , \psi = \sum_{k=0}^{+\infty} w_k q^k, \tag{3.21}$$

ϕ and ψ are analytic in $q \in \big[0, a\big)$. We also assume two smooth functions $f(\phi)$ and $g(\phi, \psi)$. The properties of homotopy derivative operator are given as:

1. $\delta_m(\phi) = u_m$
2. $\delta_m(\dot{\phi}) = \dot{u}_m$
3. $\delta_m(\phi + \psi) = \delta_m(\phi) + \delta_m(\psi)$
4. $\delta_m(\phi\psi) = \sum_{k=0}^{m} u_k w_{m-k}$
5. $\delta_m(\phi^{n+1}) = \sum_{k=0}^{m} u_{m-k}\delta_k(\phi^n)$
6. $\delta_m(f(\phi)) = \sum_{k=0}^{m-1} \big(1 - \frac{k}{m}\big) u_{m-k} \frac{\partial}{\partial u_0}\big(\delta_k(f(\phi))\big) \ , \ \delta_0(f(\phi)) = f(u_0)$
7. $\delta_m(g(\phi, \psi)) = \sum_{k=0}^{m-1} \big(1 - \frac{k}{m}\big) u_{m-k} \frac{\partial}{\partial u_0}\big(\delta_k(g(\phi, \psi))\big) +$
   $\sum_{k=0}^{m-1} \big(1 - \frac{k}{m}\big) w_{m-k} \frac{\partial}{\partial w_0}\big(\delta_k(g(\phi, \psi))\big) \ , \quad \delta_0(g(\phi, \psi)) = g(u_0, w_0)$

The use of the properties on an arbitrary nonlinear operator, N is shown below. Assume a nonlinear governing equation with states u and w.

$$N : \dot{u} + u^2 + u\sin(w) = 0 \tag{3.22}$$

We assume that u and w have the Homotopy-Maclaurin series solutions given by ϕ and ψ respectively. We write the general governing equation by substituting the states by their Homotopy-Maclaurin series solutions.

$$N : \dot{\phi} + \phi^2 + \phi\sin(\psi) = 0 \tag{3.23}$$

The application of the 3^{rd} order homotopy derivative operator on the nonlinear equation is shown below. Using the 3^{rd} property, we obtain:

$$\delta_3(\dot{\phi} + \phi^2 + \phi\sin(\psi)) = \delta_3(\dot{\phi}) + \delta_3(\phi^2) + \delta_3(\phi\sin(\psi)) \tag{3.24}$$

The first term on the right hand side of Eq. (3.24) can be calculated by applying the 2^{nd} property mentioned above. Hence we obtain, $\delta_3(\dot{\phi}) = \dot{u}_3$. The 5^{th} property can be used to calculate the second term on the right hand side of Eq. (3.24) as follows:

$\delta_3(\phi^2) = \sum_{k=0}^{2} u_{3-k}\delta_k(\phi)$

$\Rightarrow \delta_3(\phi^2) = u_3\delta_0(\phi) + u_2\delta_1(\phi) + u_1\delta_2(\phi) + u_0\delta_3(\phi)$

$\Rightarrow \delta_3(\phi^2) = 2u_3u_0 + 2u_1u_2$

Since the last term on the right hand side of Eq. (3.24), is a function of two homotopy series solutions, we use the 7^{th} property as follows:

$\delta_3(\phi\sin(\psi)) = \sum_{k=0}^{2}\left(1-\frac{k}{3}\right)u_{3-k}\frac{\partial}{\partial u_0}(\delta_k(\phi\sin(\psi)) + \sum_{k=0}^{2}\left(1-\frac{k}{3}\right)w_{3-k}\frac{\partial}{\partial w_0}(\delta_k(\phi\sin(\psi))$

$\Rightarrow \delta_3(\phi\sin(\psi)) = u_3\frac{\partial}{\partial u_0}\left[\delta_0(\phi\sin(\psi))\right] + \frac{2}{3}u_2\frac{\partial}{\partial u_0}\left[\delta_1(\phi\sin(\psi))\right] + \frac{1}{3}u_1\frac{\partial}{\partial u_0}\left[\delta_2(\phi\sin(\psi))\right] +$
$w_3\frac{\partial}{\partial w_0}\left[\delta_0(\phi\sin(\psi))\right] + \frac{2}{3}w_2\frac{\partial}{\partial w_0}\left[\delta_1(\phi\sin(\psi))\right] + \frac{1}{3}w_1\frac{\partial}{\partial w_0}\left[\delta_2(\phi\sin(\psi))\right]$

$\Rightarrow \delta_3(\phi\sin(\psi)) = \frac{1}{3}\left[2w_2(u_1\cos(w_0) - u_0w_1\sin(w_0))\right] - \frac{1}{3}\left[u_1\left(\frac{1}{2}\sin(w_0)w_1^2 - w_2\cos(w_0)\right)\right] +$
$\frac{1}{3}w_1\left[\frac{1}{2}\left(w_1u_1\sin(w_0) + u_0w_1\cos(w_0)\right) - u_2\cos(w_0) + u_0w_2\sin(w_0) + \frac{1}{2}\left(u_1w_1\sin(w_0)\right)\right] +$
$u_3\sin(w_0) + u_0w_3\cos(w_0) + \frac{1}{3}\left[2u_2w_1\cos(w_0)\right]$

It can be seen that for a non-linear problem, the above-mentioned properties when applied to the governing equations lead to recursive series expansions. This increases the size of the m^{th} order deformation equations and results in high computational requirements.

3.1.2 HAM Solution for an Example Boundary Value Problem

For solving a BVP using HAM, we first formulate the given problem as an initial value problem. The known initial boundary conditions from Eq. (3.4) are used in the selection of the initial guess as detailed later in Section 3.2. For the states and costates with unknown initial boundary conditions, we assume their values to be finite parameters β_1, β_2,....β_n. After obtaining the series solutions for each state and

costate, we use the given terminal boundary conditions to obtain corrections for the values of the finite parameters β_1, β_2,....β_n.

3.1.3 Problem Formulation for a Non-Linear Optimal Control Problem

The process can be understood with the help of a simple optimal control problem explained below. The objective functional is given by

$$\text{Min J} = \int_0^1 (x^2 + u^2)dt \tag{3.25}$$

with the governing equation

$$\dot{x} = u,\ x(0) = 1,\ t \in [0, 1] \tag{3.26}$$

where x is the state and u is the control variable.
On applying the Euler-Lagrange theorem, we obtain the following TPBVP,

$$\begin{gathered} \dot{x} + \lambda = 0,\ \dot{\lambda} + x = 0 \\ x(0) = 1,\ \lambda(1) = 0 \end{gathered} \tag{3.27}$$

where λ is the costate. The simple optimal control problem has a closed form analytical solution given by Eq. (3.28)

$$\begin{aligned} x(t) &= \frac{e^t + e^2 e^{-t}}{1 + e^2} \\ \lambda(t) &= -\frac{e^t - e^2 e^{-t}}{1 + e^2} \end{aligned} \tag{3.28}$$

Using HAM theory, a Homotopy-Maclaurin series for the state and costate is formulated as:

$$\begin{aligned} \phi(t; q) &= x_0(t) + \sum_{m=1}^{+\infty} x_m(t) q^m, q \in [0, 1] \\ \psi(t; q) &= \lambda_0(t) + \sum_{m=1}^{+\infty} \lambda_m(t) q^m, q \in [0, 1] \end{aligned} \tag{3.29}$$

where x_0 and λ_0 are the initial guesses for the state and costate respectively. x_m and λ_m can be obtained by integrating the m^{th} order deformation equations given by

$$\begin{aligned} L[x_m(t) - \chi_m x_{m-1}(t)] &= c_o H_a \delta_{m-1}(N_1[t, \phi(t; q)]) \\ L[\lambda_m(t) - \chi_m \lambda_{m-1}(t)] &= c_o H_a \delta_{m-1}(N_2[t, \psi(t; q)]) \end{aligned} \tag{3.30}$$

subject to

$$\begin{aligned} x_m(0) &= 0 \\ \lambda_m(0) &= 0 \end{aligned} \tag{3.31}$$

Substituting the state and costate by its Homotopy-Maclaurin series solution in the governing equations, we obtain:

$$\begin{aligned} N_1 &: \dot{\phi} + \psi = 0 \\ N_2 &: \dot{\psi} + \phi = 0 \end{aligned} \tag{3.32}$$

We apply the properties (1), (2), and (3) mentioned in Section 3.1.1 on the governing equations, N_1 and N_2, to obtain the right hand side of the m^{th} order deformation (Eq. (3.30)) as follows

$$\begin{aligned} \delta_{m-1}(\dot{\phi} + \psi) &= \dot{x}_{m-1} + \lambda_{m-1} \\ \delta_{m-1}(\dot{\psi} + \phi) &= \dot{\lambda}_{m-1} + x_{m-1} \end{aligned} \tag{3.33}$$

A M^{th} order series solution for the state and costate variable is represented as

$$\begin{aligned} x(t) &= x_0(t) + \sum_{m=1}^{M} x_m(t) \\ \lambda(t) &= \lambda_0(t) + \sum_{m=1}^{M} \lambda_m(t) \end{aligned} \tag{3.34}$$

3.2 Selection of Initial Guess, Linear Operator, & Auxiliary Function

Although, there are no conclusive proofs and rigorous theories to select the initial guess, the linear operator, and the auxiliary function, HAM literature provides suggestions for their selection [23]. Dr. Liao suggests to start by defining a set of basis functions which can represent the series solution of Eq. (3.3). A typical HAM series solution can be represented as a power series given by

$$u(t) = \sum_{m=0}^{+\infty} a_m e_m(t) \tag{3.35}$$

where a_m are the finite coefficients obtained by applying the Homotopy Analysis Method, and $e_m(t)$ are the basis functions chosen by the designer to represent the series solution. Eq. (3.35) is known as the *rule of solution expression*. The initial guess, linear operator, and the auxiliary function are chosen in such a way so that they satisfy the *rule of solution expression* as explained below.

3.2.1 Initial Guess

HAM literature suggests that the initial guess must be chosen such that it can be expressed by the sum of the basis functions defined above. Also, the initial guess for a state must satisfy the maximum possible number of boundary conditions for that state. Eq. (3.36) shows a typical representation of the initial guess for a state

$$x_0(t) = \sum_{m=0}^{n} b_m e_m(t) \tag{3.36}$$

where n is the number of boundary conditions on the state, b_m are the finite coefficients chosen by the designer to satisfy the boundary conditions, and $e_m(t)$ are the basis functions chosen to represent the series solution.

3.2.2 Linear Operator

The linear operator must be chosen such that the solution of Eq. (3.37) is expressed as the sum of the basis functions chosen earlier and is given by Eq. (3.38)

$$L[w(t)] = 0 \tag{3.37}$$

$$w(t) = \sum_{m=0}^{K_1} d_m e_m(t) \tag{3.38}$$

where, d_m are the finite coefficients and K_1 is a positive integer. There is no strict rule to select the value of K_1, but it is suggested that in most of the problems, it is chosen as the highest order of derivative of the original Eq. (3.3). As already mentioned in

Section 3.1, the auxiliary function for the finite interval BVPs is chosen to be 1. A detailed explanation supporting this assumption is provided later in Section 3.2.

Using Eq. (3.13), the original Eq. (3.3) is converted into an infinite number of linear subproblems governed by the m^{th} order deformation Eq. (3.18). For each value of m =1,2,3,...∞, the m^{th} order deformation equation can be solved to give analytical expressions for $u_m(t)$. Dr. Liao also defines a *rule of solution existence* as, "the initial guess, linear operator, and the auxiliary function should be chosen such that the all of the higher order(m^{th}) deformation equations are closed and have solutions". Hence, the guidelines above play an important role for guiding us to choose the initial guess, linear operator, and the auxiliary function.

3.2.3 Selection of Initial Guess, Linear Operator, and Auxiliary Function for the OCP

Since a real function can be represented by different basis functions, there may be different kinds of rule of solution expressions, and all might give accurate solutions for the non-linear problem. For the current problem, we use the simplest *rule of solution expression*, a polynomial power series for a state x, given by Eq. (3.40) for which the set of basis functions is the following set e_m

$$e_m(t) = [0, 1, t, t^2, t^3....] \tag{3.39}$$

$$x(t) = a_1 + a_2 t + a_3 t^2 + ... \tag{3.40}$$

where $a_1, a_2,$ and a_3 are the coefficients of the series solution. The approach mentioned in Section 3.2.1 is used to select the initial guesses for the state and costate. For convenience, we decide to select the initial guesses which satisfy only the initial boundary conditions for both the state and the costate. This assumption results in $n = 1$ for the initial guess. Hence, for both the state and costate, we define the initial guesses as:

$$\begin{aligned} x_0(t) &= \sum_{m=0}^{1} b_{1m} e_m(t) = b_{11}e_1 + b_{12}e_2 \\ \lambda_0(t) &= \sum_{m=0}^{1} b_{2m} e_m(t) = b_{21}e_1 + b_{22}e_2 \end{aligned} \tag{3.41}$$

To satisfy the initial boundary condition on the state, we choose $b_{11} = 0$ and $b_{12} = 1$. Since the initial boundary condition for the costate is unknown, we assume it to be some finite value β_1 as explained in Section 3.1.2. For the costate, we select $b_{22} = \beta_1$ and $b_{21} = 0$ to satisfy the initial boundary condition. We obtain the initial guesses for the state and costate as:

$$\begin{aligned} x_0(t) &= 1 \\ \lambda_0(t) &= \beta_1 \end{aligned} \tag{3.42}$$

For the linear operator, we use the approach described in Section 3.2.2 to define w(t) as shown in Eq. (3.43). The value of K_1 is 1 since the highest order derivative for both the original governing equations is 1. We can now define w(t) described in Section 3.2.1, as

$$w(t) = \sum_{m=0}^{1} d_m e_m = d_0 e_0 + d_1 e_1 = d_1 \tag{3.43}$$

The linear operator is chosen such that it satisfies Eq. (3.37) as follows:

$$L(w(t)) = \frac{d}{dt}(d_1) = 0 \tag{3.44}$$

Using Eq. (3.30) and Eq. (3.33), the m^{th} order deformation equations can now be written for the state and costate as

$$\begin{aligned} x_m(t; c_o) &= \chi_m x_{m-1}(t) + c_o \int_0^t H_a \delta_{m-1}(\dot{x} + \lambda) dt + C_1 \\ \lambda_m(t, c_o) &= \chi_m \lambda_{m-1}(t) + c_o \int_0^t H_a \delta_{m-1}(\dot{\lambda} + x) dt + C_2 \end{aligned} \qquad m\text{=}1,2,3,... \tag{3.45}$$

C_1 and C_2 are constants of integration determined by the initial conditions given by Eq. (3.31). Using the *rule of solution expression* given by Eq. (3.40) and Eq. (3.45), the auxiliary function H_a should be of the form t^{κ}. When $\kappa \leq -1$, the solutions of m^{th} order deformation Eq. (3.45) contain the terms log(t), which disobeys the *rule of*

solution expression, and when $\kappa \geq 1$, the basis function t^{κ} disappears in the solution expression given in Eq. (3.40) so that the coefficient of the term t cannot be modified even if the order of approximation tends to infinity. Hence, we set $\kappa = 0$, resulting in $H_a(t) = 1$.

3.3 Auxiliary Convergence Control Parameter

HAM guarantees the convergence of the series solution [26], which counts as one of the major advantages for using it to solve BVPs. MATLAB's symbolic toolbox is used to solve Eq. (3.45). We obtain terms for x_m and λ_m and substitute them into Eq. (3.34). Upon simplifying Eq. (3.34), we obtain a family of series solutions in c_o. The solutions for state and costate are functions of the independent variable t and c_o. The Homotopy Analysis Method provides us the freedom to choose the value of the c_o to adjust the region and the rate of convergence. Dr. Liao suggested to plot the curves of physical quantities like $\dot{x}|_{t=t'}$, $\ddot{x}|_{t=t'}$ with c_o to study their dependency on c_o, where t' can be any instant of time in the domain of the problem. These curves are termed the $c_o \sim$ curves and are denoted as $\dot{x} \sim c_o$ and $\ddot{x} \sim c_o$ for any state or physical quantity. According to the convergence theorem of HAM [55], all convergent series of $\dot{x}$ and $\ddot{x}$ converge to constant values for a specific range (R_{c_o}) of c_o values, resulting in a horizontal line in the $c_o \sim$ curves. Regardless of the initial guess, and for any value of c_o in that specific region, we will always obtain the same value of the physical quantity and the series solution is known to converge.

3.4 Discrete Squared Residual

HAM theory defines the squared residual as a measure of how well the power series satisfies the governing equations integrated over the whole domain. The squared residual for any governing equation is defined as

$$E_m(c_o) = \int_0^a \left\{ N[\sum_{n=1}^{m} u_m(t, c_o)] \right\}^2 dt \tag{3.46}$$

where a is the final value of time interval used in Eq. (3.3), E_m is the squared residual error for the governing equation, obtained at m^{th} order series solution. The convergence control parameter, c_o, plays an important role in determining the residual error for any series solution. As proposed by Liao [21], once we decide the specific range of c_o (described in Section 3.3) for which the series converges, we can find the optimal value of c_o within that range by minimizing the squared residual error.

Due to the high computational requirements in E_m, theory also defines a discrete squared residual E_{md} for the m^{th} order series solution as

$$E_{md} = \frac{1}{N_{step}+1} \sum_{j=0}^{N_{step}} \left\{ \Delta_m(\tau_j; c_o) \right\}^2, \ \tau_j = \frac{t_f j}{N_{step}} \tag{3.47}$$

where

$$\Delta_m(\tau; c_o) = N(u_m(\tau; c_o)) \tag{3.48}$$

N_{step} is the number of time steps used, and t_f is the final time of the OCP. For the current study, N_{step} is assumed to be 40. An overall discrete squared residual $E_{md,total}$ can be defined by adding the discrete squared residuals for each governing equation as follows

$$E_{md,total} = E_{md,N_1} + E_{md,N_2} + E_{md,N_3} + ... \tag{3.49}$$

where E_{md,N_1} is the discrete squared residual for the governing equation N_1.

3.5 Results for the Optimal Control Problem

The m^{th} order deformation Eq. (3.45) is solved to obtain the analytical terms for x_m and λ_m terms in c_o and β_1. First, we assume the value of c_o to be -1. Then, we use the final boundary condition on the costate to obtain a non-linear equation which can be root solved for β_1. Using the value of β_1, we can obtain m^{th} order series solutions for both the state and costate.

Further, we plot the $c_0 \sim$ curves to understand the convergence properties of the state and costate series solutions. For this test case, we used the quantities $x \sim c_o$, $\dot{x} \sim c_o$, $\ddot{x} \sim c_o$ for the state and $\lambda \sim c_o$, $\dot{\lambda} \sim c_o$, $\ddot{\lambda} \sim c_o$ for the costate. Since the curves converge at each instant of time, we chose to plot them at the final time of 1 s. Figs. 3.1(a) and 3.1(b) show the $c_o \sim$ curves for the 3^{rd} order and 5^{th} order series solutions respectively. It was found that for the 5^{th} order solution, a common range in c_o could be found for both the state and the costate in which the curves converge to constant values for all the mentioned physical quantities. This common range was identified to be [-1.2, 0] for the 5^{th} order solution. The convergence region increases with an increase in the order of solution, giving designers more freedom in choice of c_o.

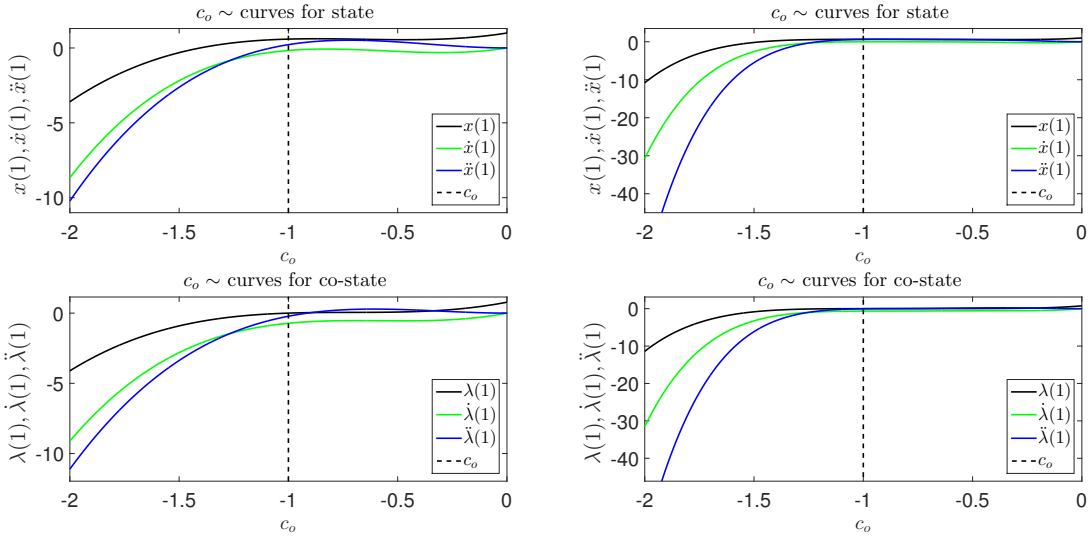

(a) 3^{rd} order $c_o \sim$ curve

(b) 5^{th} order $c_o \sim$ curve

Figure 3.1.: $c_o \sim$ curves for the simple optimal control problem.

We minimize the total discrete squared residual given by Eq. (3.49), to obtain the optimal c_o for the 5^{th} order solution. MATLAB's *fminbnd* function based on the Golden Section Search Algorithm with parabolic interpolation was used to minimize $E_{md,total}$ for the range [-1.2, 0]. The optimal value of c_o for the 5^{th} order solution

was found to be -0.9567. The optimal c_o is used again to obtain the series solutions for the state and costate. β_1 is root solved again by using the terminal boundary condition on the costate. This method of using an updated value of c_o to obtain the series solutions is known as "convergence control".

Since the initial assumed value of $c_o = -1$ already lies in the horizontal range as shown in Fig. 3.1(b), convergence control wasn't necessary in this simple case. However, to further reduce the total discrete squared residual, it is good practice to use the optimal value of c_o. Table 3.1 shows the difference between the total discrete squared residual obtained by using an optimal value of c_o.

Table 3.1: Effect of c_o on total discrete squared residual.

c_o	$E_{md,Total}$
-1	3.17×10^{-5}
-0.9567	1.27×10^{-6}

Fig. 3.2(a) shows the total discrete squared residual at several orders of solution for a very short range of c_o, in which most of the optimal values of c_o lie. It can also be seen that, as the order of solution increases, the optimal c_o shifts towards the value of -1. In literature, for a number of boundary value problems solved using HAM, $c_o = -1$ is reported to lie in the horizontal range for the physical quantities, but this may not be true for boundary value problems in general. The total discrete squared residual decreases with an increase in order as seen in Fig. 3.2(b). The computations were performed on the Intel(R) Xeon(R) CPU-E3-1225 v3 3.20 Ghz (4 CPUs) processor. CPU times increases almost linearly with the order of solution as seen from Fig. (3.3).

The series solutions for both the state and costate are compared with the analytical solution as shown in the Fig. 3.4. The series solutions without convergence control ($c_o = -1$) are also compared with the solutions obtained using the optimal c_o.

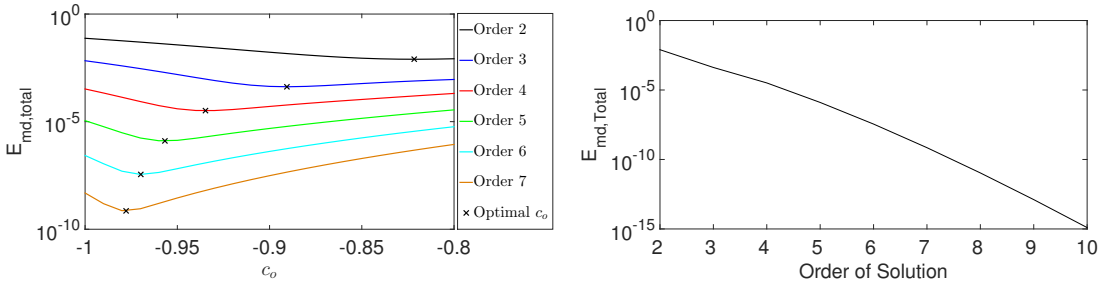

(a) Optimal c_o for several orders of solution

(b) $E_{md,Total}$ vs order of solution

Figure 3.2.: Total discrete squared residual for the simple optimal control problem.

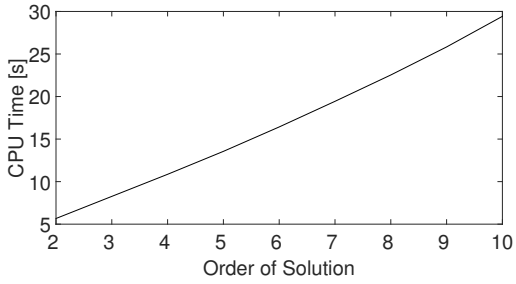

Figure 3.3.: CPU time with order of solution for the simple optimal control problem.

Although, both of the values of c_o lie in the convergence region, a small improvement is obtained by using the optimal value of c_o. The initial guess for the state variable was chosen to be 0, and does not change with c_o. For the test case, the 5^{th} order series solution is represented as

$$\begin{aligned} x(t) &= 1 - 0.76t + 0.5t^2 - 0.12t^3 + 0.04t^4 - 0.01t^5 \\ \lambda(t) &= 0.76 - t + 0.38t^2 - 0.16t^3 + 0.03t^4 - 0.01t^5 \end{aligned} \tag{3.50}$$

A number of different initial guesses were also used to compute the HAM series solution. Table 3.2 shows the total discrete squared residual obtained at 5^{th} order HAM solution for the initial guesses used. It must be noted that for each of the guess, initial boundary conditions on both the state and costate are satisfied. The initial guess given in the last row is based on an exponential *rule of solution expression*.

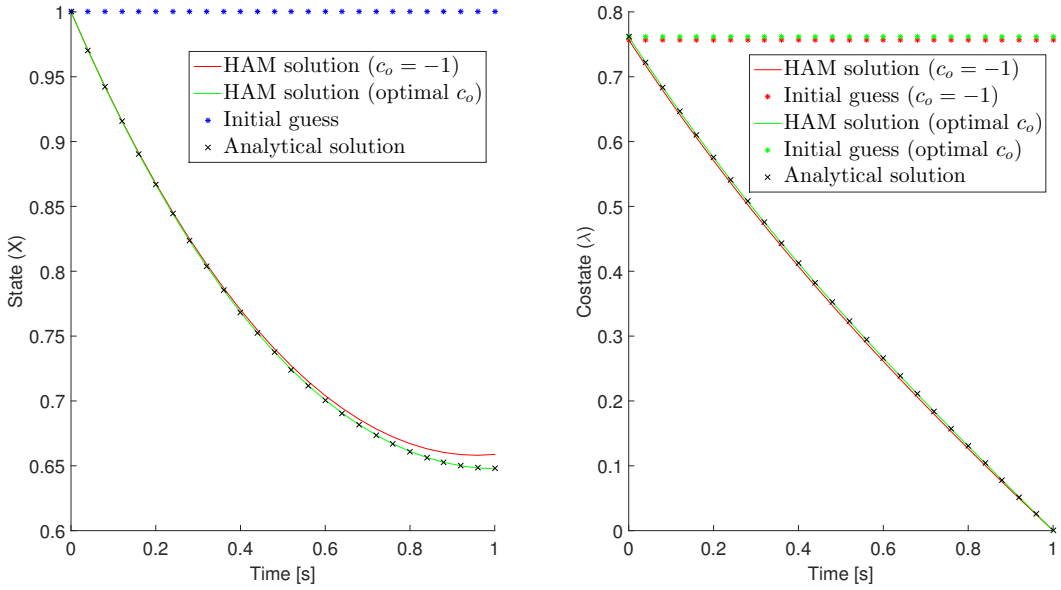

Figure 3.4.: State and costate 5^{th} order HAM solution for the simple optimal control problem.

Since the analytical solution of the problem (Eq. (3.28)) contains exponential terms, it can be concluded that using an exponential series *rule of solution expression* is apt for this particular problem. This fact is also confirmed by the least value of total discrete squared residual obtained by using the exponential initial guess as compared to other initial guesses.

Table 3.2: Flexibility of initial guess on simple control problem.

Initial Guess $[x_0, \lambda_0]$	$E_{md,Total}$
$[1, \beta_1]$	1.27×10^{-6}
$[1, \beta_1(1-t)]$	1.90×10^{-6}
$[1, \beta_1 e^t]$	1.37×10^{-5}
$[e^t, \beta_1 e^t]$	1.41×10^{-8}

3.6 Cook-Book for HAM approach to TPBVPs

A step by step formal approach for solving TPBVPs using HAM is provided below.

1. Formulate the TPBVP with the set of governing equations and the boundary conditions by using the Euler-Lagrange equations.

2. Check the initial conditions for all the state and costate variables. For all states and costates with unknown initial conditions, assume those to be unknown parameters, β_1, β_2,.. ,β_n.

3. For the free final-time TPBVP, assume the final time to be another unknown parameter, t_f.

4. Use the HAM guidelines to build the initial guess, linear operator, and the auxiliary function for each governing equation and state and costate variables.

5. Solve the m^{th} order deformation equations for each governing equation using a symbolic computation algebra system to obtain the M^{th} order series solutions for states and costates in terms of β_i, t_f and c_o. Assume c_o to be initially -1.

6. For the finite time interval problem, apply the n terminal boundary conditions on the series solutions to obtain a non-linear system of equations in β_1, β_2,.. ,β_n. For the free time interval problem, use the n terminal boundary conditions on the state and costate variables as well as the transversality condition to obtain a nonlinear system of equations in n+1 variables. MATLAB's Fsolve function is then used to numerically solve the non-linear system of equations obtained. If the system results in multiple solutions for the unknown parameters, then series solutions are constructed for each set of parameters. The set of parameter for which the objective function is minimum is chosen.

7. Using the series solutions obtained, plot the $c_o \sim$ curves for various physical quantities like $\dot{x}$, $\ddot{x}$ for each state and costate variable whose series solution is not a constant value.

8. Find a common range of c_o for which the various physical quantities converge to constant values. The common range can be identified by horizontal regions in the $c_o \sim$ curves.

9. Select any value of c_o from that common range. We can also find the optimal value of c_o by minimizing the total discrete squared residual within that range. For problems with no common range available, we can minimize the total discrete squared residual on the real number range, $(-\infty, +\infty)$, to obtain the optimal c_o.

10. Use the updated (optimal) value of c_o to repeat step 6 and find the final M^{th} order HAM series solutions for the states and costates.

11. As already explained before, steps 6-10 are referred to as the "convergence control" in the HAM literature.

12. Visual comparison of the M^{th} order solution is done with the $(M-1)^{th}$ order solution. The process is terminated, if significant changes in the state and costate solutions can't be observed. If the designer chooses to continue, higher order HAM solutions are computed.

Fig. 3.5 shows the various steps followed in the HAM approach to solve indirect trajectory optimization problems in the form of a flow chart.

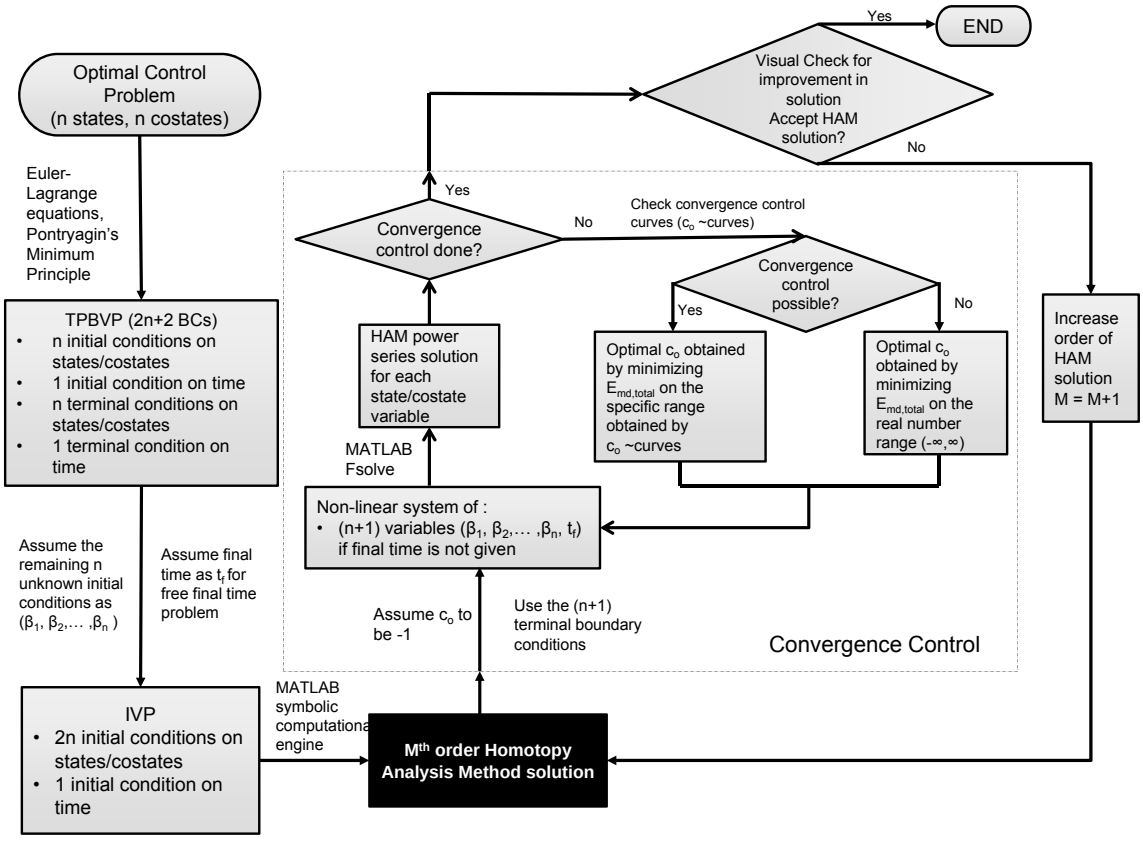

Figure 3.5.: Flowchart showing the HAM process

3.7 HAM Based Solver Packages

A number of Homotopy analysis method based packages has been developed in the past for solving non-linear boundary value problems arising in science and engineering. Some of the popular open source packages like BVPh [56] and APOh [57] are based on the symbolic algebra system of Mathematica [58] and Maple [59]. Bvph 2.0 provides the flexibility of using multiple convergence control paramters, can handle singularities, and is capable of solving nonlinear multi-point boundary value and eigenvalue problems. It also gives the flexibility of approximating the right hand side

of the m^{th} order deformation equations by the use of Chebyshev and hybrid-base polynomials.

4. HOMOTOPY ANALYSIS METHOD APPLIED TO TRAJECTORY OPTIMIZATION PROBLEMS

In this chapter, the HAM approach to solve OCPs described previously is applied to more realistic optimal control problems. Two optimal control problems are formulated as indirect trajectory optimization problems, and solutions obtained from the HAM approach are compared with those obtained from MATLAB's *bvp4c* function. The first part of this chapter discusses Zermelo's problem while the second part discusses a classical 2D ascent problem of a lunar ascent vehicle launching from the surface of the Moon to a circular orbit at 185.2 km. Additionally, a modified fixed final time 2D ascent problem is also investigated to differentiate the solution approach between the two types of problems. The effect of using the convergence control is found to be negligible for these problems, and possible reasons that support this observation are provided. It is also found that the modified fixed final time 2D ascent problem has better convergence properties as compared to the classical 2D ascent problem since an extra parameter of optimal final time has to be solved for in the latter case.

4.1 Zermelo's Problem

Zermelo's problem [60] consists of minimizing the time required by a boat to cross a river. Fig. 4.1 shows a schematic of the optimal control problem. θ is the boat steering angle from the horizontal direction which is varied continuously to reach the terminal point across the river in the minimum possible time. The boat is assumed to move with a constant velocity, V of 1 m/s.

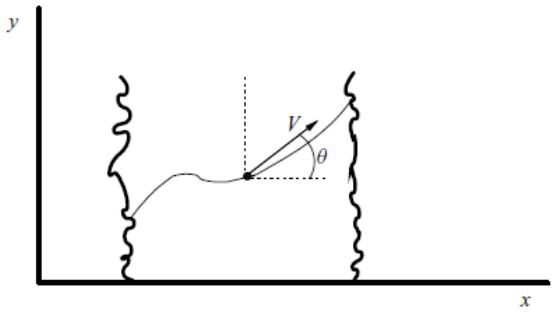

Figure 4.1.: Schematic for Zermelo's problem [60].

The objective function, J, is defined as

$$\text{Min } J = t_f \tag{4.1}$$

with the dynamics

$$\begin{aligned} \dot{x} &= x + V\cos\theta \\ \dot{y} &= y + V\sin\theta \end{aligned} \tag{4.2}$$

where, the states x and y are the horizontal and vertical coordinates respectively. It must be noted that the dynamics are modified to include river currents x and y, both in the horizontal and vertical directions. The Hamiltonian is defined as

$$\mathscr{H} = \lambda_x(x + V\cos\theta) + \lambda_y(y + V\sin\theta) \tag{4.3}$$

where λ_x and λ_y are the costates corresponding to the two states. We use the Euler-Lagrange theorem to obtain the dynamics for the costates given in Eq. (4.4). The control law is obtained in Eq. (4.5) which can also be written with a negative sign as shown in Eq. (4.6)

$$\begin{aligned} \dot{\lambda}_x &= -\lambda_x \\ \dot{\lambda}_y &= -\lambda_y \end{aligned} \tag{4.4}$$

$$\tan\theta = \frac{\lambda_y}{\lambda_x} \tag{4.5}$$

$$\tan\theta = \frac{\lambda_y}{\lambda_x} = \frac{-\lambda_y}{-\lambda_x} \tag{4.6}$$

The boat starts from (0,0) and crosses the river to reach (1,1). The set of boundary conditions along with the transversality condition obtained for final time are given in Eq. (4.7).

$$\begin{aligned} x(0) = 0,\ y(0) = 0 \\ x(t_f) = 1,\ y(t_f) = 1 \\ \mathscr{H}_{t_f} = -1 \end{aligned} \tag{4.7}$$

Since the control law can have both the positive and negative signs (Eq. (4.6)), it cannot distinguish the quadrant in which the angle θ resides. Hence, we obtain the values of $\cos\theta$ and $\sin\theta$ in Eq. (4.8)

$$\begin{aligned} \cos\theta &= \frac{\pm\lambda_x}{\sqrt{\lambda_x^2 + \lambda_y^2}} \\ \sin\theta &= \frac{\pm\lambda_y}{\sqrt{\lambda_x^2 + \lambda_y^2}} \end{aligned} \tag{4.8}$$

We use the Legendre-Clebsch condition (Eq. (2.9)) in Eq. (4.9) and Eq. (4.10) to pick the negative sign for the terms obtained in Eq. (4.8)

$$\mathscr{H}_{\theta\theta} = -\lambda_x V\cos\theta - \lambda_y V\sin\theta \tag{4.9}$$

$$\mathscr{H}_{\theta\theta} = -\lambda_x V\left(\frac{\pm\lambda_x}{\sqrt{\lambda_x^2 + \lambda_y^2}}\right) - \lambda_y V\left(\frac{\pm\lambda_y}{\sqrt{\lambda_x^2 + \lambda_y^2}}\right) \tag{4.10}$$

Substituting the terms from Eq. (4.8) into the governing equations, we obtain Eq. (4.11).

$$\begin{aligned} \dot{x} - x + V\left(\frac{\lambda_x}{\sqrt{\lambda_x^2 + \lambda_y^2}}\right) = 0 \\ \dot{y} - y + V\left(\frac{\lambda_y}{\sqrt{\lambda_x^2 + \lambda_y^2}}\right) = 0 \\ \dot{\lambda_x} + \lambda_x = 0 \\ \dot{\lambda_y} + \lambda_y = 0 \end{aligned} \tag{4.11}$$

4.1.1 HAM Problem Formulation

The Homotopy-Maclaurin series and the m^{th} order deformation equations for the states and costates are given by Eq. (4.12) and Eq. (4.13).

$$\begin{aligned}
\phi_x(t;q) &= x_0(t) + \sum_{m=1}^{+\infty} x_m(t)q^m \\
\phi_y(t;q) &= y_0(t) + \sum_{m=1}^{+\infty} y_m(t)q^m \\
\psi_{\lambda_x}(t;q) &= \lambda_{x_0}(t) + \sum_{m=1}^{+\infty} \lambda_{x_m}(t)q^m \\
\psi_{\lambda_y}(t;q) &= \lambda_{y_0}(t) + \sum_{m=1}^{+\infty} \lambda_{y_m}(t)q^m
\end{aligned} \tag{4.12}$$

$$\begin{aligned}
L[x_m(t) - \chi_m x_{m-1}(t)] &= c_o H_a \delta_{m-1}(N_1[t, \phi_x(t;q)]) \\
L[y_m(t) - \chi_m y_{m-1}(t)] &= c_o H_a \delta_{m-1}(N_2[t, \phi_y(t;q)]) \\
L[\lambda_{x_m}(t) - \chi_m \lambda_{x_{m-1}}(t)] &= c_o H_a \delta_{m-1}(N_3[t, \psi_{\lambda_x}(t;q)]) \\
L[\lambda_{y_m}(t) - \chi_m \lambda_{y_{m-1}}(t)] &= c_o H_a \delta_{m-1}(N_4[t, \psi_{\lambda_y}(t;q)])
\end{aligned} \tag{4.13}$$

where $q \in [0,1]$, x_0, y_0, λ_{x_0} and λ_{y_0} are the initial guesses, subject to

$$\begin{aligned}
x_m(0) = 0,\ y_m(0) = 0 \\
\lambda_{x_m}(0) = 0,\ \lambda_{y_m}(0) = 0
\end{aligned} \tag{4.14}$$

The Homotopy-Maclaurin series expansions for the states and costates are substituted into the Eq. (4.11) to obtain Eq. (4.15).

$$\begin{aligned}
N_1 : \dot{\phi_x}\sqrt{\psi_{\lambda_x}^2 + \psi_{\lambda_y}^2} - \phi_x\sqrt{\psi_{\lambda_x}^2 + \psi_{\lambda_y}^2} + \psi_{\lambda_x} = 0 \\
N_2 : \dot{\phi_y}\sqrt{\psi_{\lambda_x}^2 + \psi_{\lambda_y}^2} - \phi_y\sqrt{\psi_{\lambda_x}^2 + \psi_{\lambda_y}^2} + \psi_{\lambda_y} = 0 \\
N_3 : \dot{\psi_{\lambda_x}} + \psi_{\lambda_x} = 0 \\
N_4 : \dot{\psi_{\lambda_y}} + \psi_{\lambda_y} = 0
\end{aligned} \tag{4.15}$$

The governing equations are simplified to avoid square root functions in the denominator. This helps in reducing the effort to apply the homotopy derivative opera-

tor properties on the equations. We apply the properties of the homotopy derivative operator on the governing equations, N_1 N_2, N_3 and N_4 to obtain the right hand side of the m^{th} order deformation equation (Eq. (4.13)) as follows

$$\begin{aligned}
\delta_{m-1}(N_1) &= \delta_{m-1}(\dot{\phi_x}\sqrt{\psi_{\lambda_x}^2+\psi_{\lambda_y}^2}) - \delta_{m-1}(\phi_x\sqrt{\psi_{\lambda_x}^2+\psi_{\lambda_y}^2}) + \lambda_{x_{m-1}} \\
\delta_{m-1}(N_2) &= \delta_{m-1}(\dot{\phi_y}\sqrt{\psi_{\lambda_x}^2+\psi_{\lambda_y}^2}) - \delta_{m-1}(\phi_y\sqrt{\psi_{\lambda_x}^2+\psi_{\lambda_y}^2}) + \lambda_{y_{m-1}} \\
\delta_{m-1}(N_3) &= \dot{\lambda}_{x_{m-1}} + \lambda_{x_{m-1}} \\
\delta_{m-1}(N_4) &= \dot{\lambda}_{y_{m-1}} + \lambda_{y_{m-1}}
\end{aligned} \tag{4.16}$$

To evaluate the right hand side terms for the first and second m^{th} order deformation equations, MATLAB based symbolic functions are built which auto-create the terms at each order for the m^{th} order deformation equations.

4.1.2 Selection of Linear Operator, Initial Guess and Auxiliary Function for Zermelo's Problem

A set of polynomial functions as the basis functions and a *rule of solution expression* similar to the one used in the previous problem given by Eq. (3.40) is chosen for Zermelo's problem. Similar to the process before, for convenience, we select the initial guesses which satisfy only the initial boundary conditions on the states and costates. We build the initial guesses for each state and costate as explained in the Section 3.2.1.

$$\begin{aligned}
x_0(t) &= \sum_{m=0}^{1} b_{1m}e_m(t) = b_{11}e_1 + b_{12}e_2 \\
y_0(t) &= \sum_{m=0}^{1} b_{2m}e_m(t) = b_{21}e_1 + b_{22}e_2 \\
\lambda_{x_0}(t) &= \sum_{m=0}^{1} b_{3m}e_m(t) = b_{31}e_1 + b_{32}e_2 \\
\lambda_{y_0}(t) &= \sum_{m=0}^{1} b_{4m}e_m(t) = b_{41}e_1 + b_{42}e_2
\end{aligned} \tag{4.17}$$

where e_m is given by Eq. (3.39). The values of the coefficients chosen for the initial guess to satisfy the initial boundary conditions are given in the Table (4.1)

Table 4.1: Coefficients and initial guess for Zermelo's problem.

j	state and costate	Coefficient b_{j1}	Coefficient b_{j2}	Initial Guess
1	x	0	0	0
2	y	0	0	0
3	λ_x	0	β_1	β_1
4	λ_y	0	β_2	β_2

To select the linear operator, we follow the same process as used in Section 3.2.3. Since, the highest order of derivative for all the governing equations is 1, we select the value of K_1 defined in Eq. (3.38) to be 1. The function w(t) can be defined as

$$w(t) = \sum_{m=0}^{1} d_m e_m = d_0 e_0 + d_1 e_1 = d_1 \tag{4.18}$$

Using Eq. (3.44), we can select the linear operator as $\frac{d}{dt}$. Following the approach we used for the previous example, we select the auxiliary function to be 1. Using Eq. (4.13) and Eq. (4.16), we can now write the m^{th} order deformation equations as given in Eq. (4.19)

$$\begin{aligned}
x_m(t;c_o) &= \chi_m x_{m-1}(t) + c_o \int_0^t \Big[\delta_{m-1}(\dot{\phi_x}\sqrt{\psi_{\lambda_x}^2+\psi_{\lambda_y}^2}) - \delta_{m-1}(\phi_x\sqrt{\psi_{\lambda_x}^2+\psi_{\lambda_y}^2}) \\
&\quad + \lambda_{x_{m-1}})\Big]dt + C_1 \\
y_m(t;c_o) &= \chi_m y_{m-1}(t) + c_o \int_0^t \Big[\delta_{m-1}(\dot{\phi_y}\sqrt{\psi_{\lambda_x}^2+\psi_{\lambda_y}^2}) - \delta_{m-1}(\phi_y\sqrt{\psi_{\lambda_x}^2+\psi_{\lambda_y}^2}) \\
&\quad + \lambda_{y_{m-1}})\Big]dt + C_2 \\
\lambda_{x_m}(t,c_o) &= \chi_m \lambda_{x_{m-1}}(t) + c_o \int_0^t (\dot{\lambda}_{x_{m-1}} + \lambda_{x_{m-1}})dt + C_3 \\
\lambda_{y_m}(t,c_o) &= \chi_m \lambda_{y_{m-1}}(t) + c_o \int_0^t (\dot{\lambda}_{y_{m-1}} + \lambda_{y_{m-1}})dt + C_4
\end{aligned} \tag{4.19}$$

where, χ_m is given by Eq. (3.16). C_1 ,C_2, C_3, and C_4 are calculated using the boundary conditions in Eq. (4.14). Since we are also required to calculate the optimal final time for the problem, another unknown parameter, t_f, is used. Following the steps defined in Section 3.6, we select the value of c_o to be -1. The terminal boundary conditions on the states and the transversality condition on the final time parameter, t_f, are applied to formulate a non-linear system of equations in the parameters β_1, β_2, and t_f. MATLAB's Fsolve function based on the default Trust-region-dogleg algorithm is used to numerically solve the non-linear system of equations. Table. 4.2 lists the settings used for the Fsolve function. Fsolve requires an initial guess for the nonlinear

Table 4.2: Fsolve settings.

Algorithm	Trust-region-dogleg
Maximum Function Evaluations	200,000
Maximum iterations	200,000
Finite difference method	Forward
Function Tolerance	10^{-6}
Step Tolerance	10^{-6}

Table 4.3: Initial guess for Fsolve function at 1^{st} order HAM solution.

Parameter	Guess
β_1	0.1
β_2	0.1
t_f	0.5

system to begin, for which an educated initial guess given in the Table 4.3 is input to calculate the unknown parameters for the 1^{st} order HAM solution. The values

obtained for 1^{st} order solution are used as the initial guess by Fsolve for the next order HAM solution.

4.1.3 Results for Zermelo's Problem

Fig. 4.2 shows the $c_o \sim$ curves of the physical quantities for all the state and costate variables at the 7^{th} order solution for $c_o \in [-2, 0]$. For the states, the plots seem to show a common range of [-1,0] in which the physical quantities converge to constant values. The common range from the $c_o \sim$ curves of costate quantities is approximated to be [-1,-0.6]. On changing the axes scales, as shown in Fig. 4.3, the values for state quantities show different convergence behavior for c_o within the domain [-1,0]. It was concluded that the convergence behavior for the state quantities in Fig. 4.2 was misleading. Due to the large magnitude of quantities in the range [-2,-1.5], the plots couldn't capture the convergence phenomena in the range [-1,0]. However, for the costate quantities, we could confirm a common convergence region of [-1,-0.6] from Fig. 4.3. Due to the fact that we couldn't find a common region of c_o for all the state and costate quantities, the use of a convergence control wasn't possible for this problem.

Since we couldn't use convergence control on the problem, we could use the assumed value of c_o of -1. An optimal c_o was determined by minimizing the total discrete squared residual over the range $[-10^{10}, 10^{10}]$. For the 7^{th} order HAM solution, Table 4.4 lists the total discrete squared residual and the parameters calculated corresponding to two c_o values. The optimal t_f from *bvp4c* is calculated to be 0.8814 s. The series solutions for the states and costates are compared with the results obtained from *bvp4c* in Fig. 4.4. As seen from Fig. 4.4, almost negligible difference in the parameters obtained from the two c_o values result in similar trajectories for the states and costates. Due to the difference in the optimal final time values obtained from the two methods, the terminal boundary conditions are not completely achieved for the solutions obtained using the HAM approach.

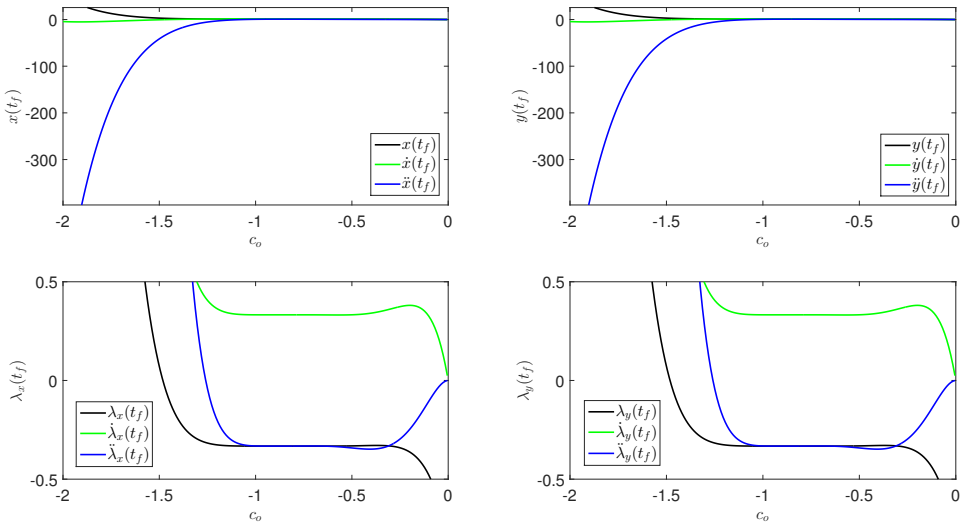

Figure 4.2.: $c_o \sim$ curves for Zermelo's problem: $c_o \in [-2, 0]$

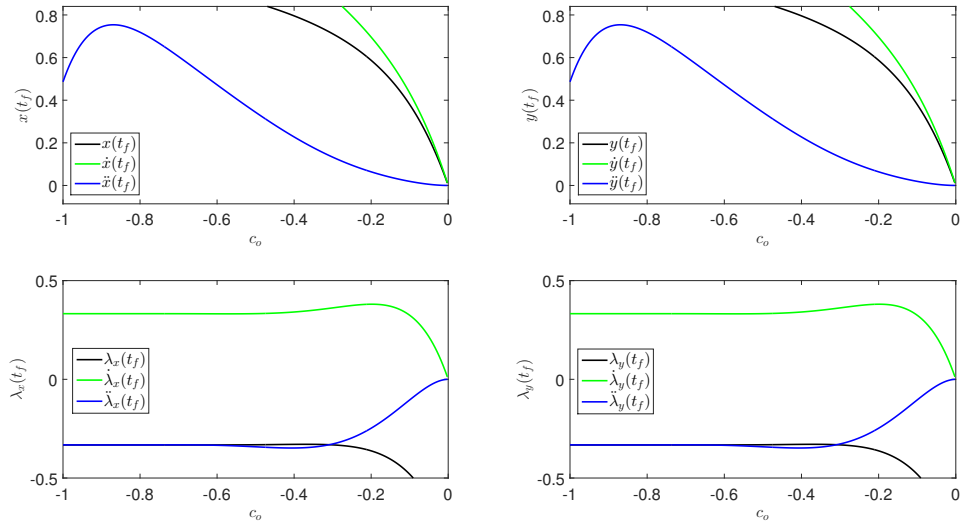

Figure 4.3.: $c_o \sim$ curves for Zermelo's problem: $c_o \in [-1, 0]$

Fig. 4.5 compares the control history obtained using the two methods. A constant steering angle of 45 deg is needed to be maintained for the boat to reach the terminal point. The control history obtained using the HAM method records a higher time as

Table 4.4: c_o values and parameter values for Zermelo's problem (7^{th} order).

c_o	$E_{md,Total}$	β_1	β_2	$t_f[s]$
-1	0.00218588	-0.81730068	-0.81730068	0.89946559
-1.0056	0.00218278	-0.81730069	-0.81730069	0.89946559

compared to the one obtained from *bvp4c*. This is due to the small difference between the optimal final time values obtained from the two methods. Figs. 4.6(a) and 4.6(b) show the total discrete squared residual and the CPU-time to solve Zermelo's problem. It can be seen that the CPU-time for the next consecutive order is almost double of the previous order value. This is due to the fact that the m^{th} order deformation equations for the next higher order consist of all the terms from the previous order solution.

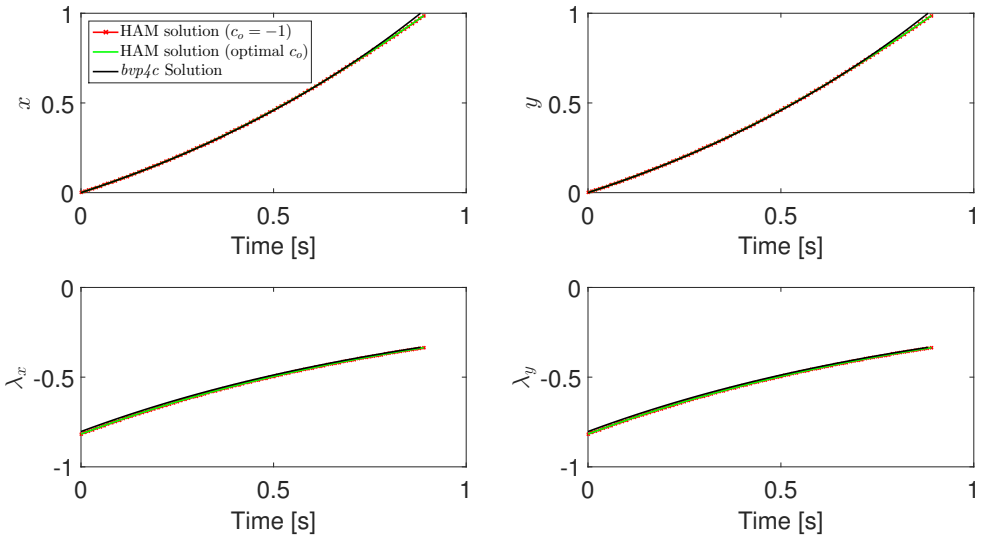

Figure 4.4.: State and costate 7^{th} order HAM solution for Zermelo's problem.

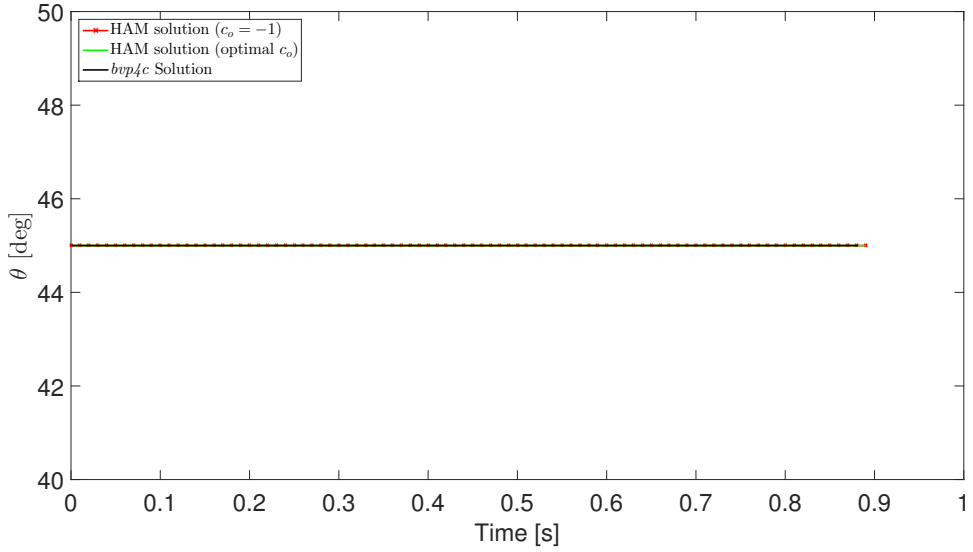

Figure 4.5.: Control history for Zermelo's problem.

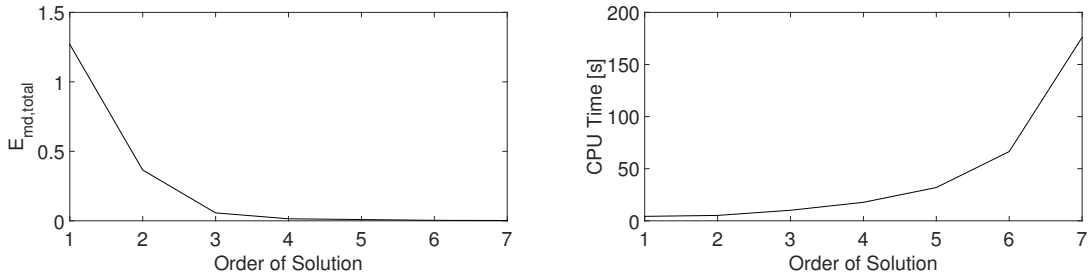

(a) $E_{md,Total}$ vs order of solution

(b) CPU time vs order of solution

Figure 4.6.: Computational performance for Zermelo's problem.

4.2 2D Ascent Launch Problem

The classical 2D ascent problem [60] consists of launching an ascent vehicle from the surface of the Moon to a circular orbit of 185.2 km in the minimum possible time. A flat Moon model is assumed as shown in Fig. 4.7.

The assumptions for the optimal control problem are:

1. The instantaneous steering angle α is the only control variable.

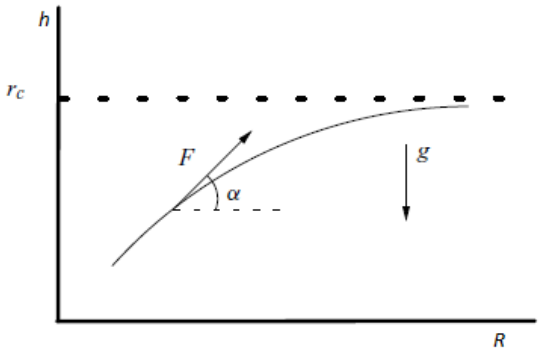

Figure 4.7.: Flat-Moon model for classical 2D ascent problem [60].

2. Acceleration due to gravity by the Moon is assumed to be 1.62 m/s^2.

3. The thrust to weight ratio for the ascent vehicle is 3.

4. Constant vehicle mass and a constant thrust force, F is assumed.

5. The final altitude to be achieved is 185.2 km.

6. There is no atmosphere present.

The objective function for the problem is defined in Eq. (4.20)

$$\text{Min } J = t_f \tag{4.20}$$

with the equations of motion given by Eq. (4.21)

$$\begin{aligned} \dot{R} &= v_x \\ \dot{h} &= v_y \\ \dot{v_x} &= \frac{F}{m}\cos\alpha \\ \dot{v_y} &= \frac{F}{m}\sin\alpha - g \end{aligned} \tag{4.21}$$

where $g = 1.62\ m/s^2$, the states R and h represent the downrange and altitude of the vehicle, and v_x and v_y are the horizontal and the vertical velocities, respectively. $\frac{F}{m}$ is the thrust acceleration of the vehicle and is calculated using Eq. (4.22).

$$\frac{F}{m} = (\text{Thrust to weight})(g) = 4.86\,\text{m/s}^2 \tag{4.22}$$

The Hamiltonian is defined in Eq. (4.23),

$$\mathscr{H} = \lambda_R(v_x) + \lambda_h(v_y) + \lambda_{v_x}\left(\frac{F}{m}\cos\alpha\right) + \lambda_{v_y}\left(\frac{F}{m}\sin\alpha - g\right) \tag{4.23}$$

where λ_R, λ_h, λ_{v_x}, and λ_{v_y} are the costates corresponding to the 4 states defined above. Using the Euler-Lagrange equations, we derive the dynamics for the costates in Eq. (4.24)

$$\begin{aligned} \dot{\lambda}_R &= 0 \\ \dot{\lambda}_h &= 0 \\ \dot{\lambda}_{v_x} &= -\lambda_R \\ \dot{\lambda}_{v_y} &= -\lambda_h \end{aligned} \tag{4.24}$$

The control law is obtained in Eq. (4.25) which can also be written with a negative sign, as shown in Eq. (4.26)

$$\tan\alpha = \frac{\lambda_{v_y}}{\lambda_{v_x}} \tag{4.25}$$

$$\tan\alpha = \frac{\lambda_{v_y}}{\lambda_{v_x}} = \frac{-\lambda_{v_y}}{-\lambda_{v_x}} \tag{4.26}$$

Since the control law obtained for the problem is same as the one derived for Zermelo's problem (Eq. (4.6)), we use the same process to obtain the values of the terms $\cos\alpha$ and $\sin\alpha$ as shown in Eq. (4.27).

$$\begin{aligned} \cos\alpha &= \frac{\pm\lambda_{v_x}}{\sqrt{\lambda_{v_x}^2 + \lambda_{v_y}^2}} \\ \sin\alpha &= \frac{\pm\lambda_{v_y}}{\sqrt{\lambda_{v_x}^2 + \lambda_{v_y}^2}} \end{aligned} \tag{4.27}$$

We use the Legendre-Clebsch condition (Eq. (2.9)) in Eq. (4.28) and Eq. (4.29) to pick the negative signs for the terms obtained in Eq. (4.27)

$$\mathscr{H}_{\alpha\alpha} = -\lambda_{v_x}\left(\frac{F}{m}\right)\cos\alpha - \lambda_{v_y}\left(\frac{F}{m}\right)\sin\alpha \tag{4.28}$$

$$\mathscr{H}_{\alpha\alpha} = -\lambda_{v_x}\frac{F}{m}\left(\frac{\pm\lambda_{v_x}}{\sqrt{\lambda_{v_x}^2+\lambda_{v_y}^2}}\right) - \lambda_{v_y}\frac{F}{m}\left(\frac{\pm\lambda_{v_y}}{\sqrt{\lambda_{v_x}^2+\lambda_{v_y}^2}}\right) \tag{4.29}$$

The updated equations of motion are given by Eq. (4.30)

$$\begin{aligned}
\dot{R} &= v_x \\
\dot{h} &= v_y \\
\dot{v_x} &= \frac{F}{m}\left(\frac{-\lambda_{v_x}}{\sqrt{\lambda_{v_x}^2+\lambda_{v_y}^2}}\right) \\
\dot{v_y} &= \frac{F}{m}\left(\frac{-\lambda_{v_y}}{\sqrt{\lambda_{v_x}^2+\lambda_{v_y}^2}}\right) - g
\end{aligned} \tag{4.30}$$

Using the transversality condition given by Eq. (2.7), we obtain the boundary conditions for the TPBVP in Table 4.5. An additional boundary condition is derived for the Hamiltonian given by, $\mathscr{H}_f = -1$.

Table 4.5: Boundary conditions - classical 2D ascent problem.

State/Costate	Initial condition	Terminal Condition
R	0 km	free
h	0 km	185.2 km
v_x	0 m/s	1.627 km/s
v_y	0 m/s	0 m/s
λ_R	free	0
λ_h	free	free
λ_{vx}	free	free
λ_{vy}	free	free

4.2.1 HAM Problem Formulation (Classical 2D Ascent)

Following the set of steps described in Section 3.5, we can begin to formulate the HAM problem by defining the Homotopy-Maclaurin series in Eq. (4.31) and the mth order deformation equations in Eq. (4.32) for each state and costate.

$$\begin{aligned}
\phi_R(t;q) &= R_0(t) + \sum_{m=1}^{+\infty} R_m(t)q^m \\
\phi_h(t;q) &= h_0(t) + \sum_{m=1}^{+\infty} h_m(t)q^m \\
\phi_{v_x}(t;q) &= v_{x0}(t) + \sum_{m=1}^{+\infty} v_{xm}(t)q^m \\
\phi_{v_y}(t;q) &= v_{y0}(t) + \sum_{m=1}^{+\infty} v_{ym}(t)q^m \\
\psi_{\lambda_R}(t;q) &= \lambda_{R_0}(t) + \sum_{m=1}^{+\infty} \lambda_{R_m}(t)q^m \\
\psi_{\lambda_h}(t;q) &= \lambda_{h_0}(t) + \sum_{m=1}^{+\infty} \lambda_{h_m}(t)q^m \\
\psi_{\lambda_{v_x}}(t;q) &= \lambda_{v_{x0}}(t) + \sum_{m=1}^{+\infty} \lambda_{v_{xm}}(t)q^m \\
\psi_{\lambda_{v_y}}(t;q) &= \lambda_{v_{y0}}(t) + \sum_{m=1}^{+\infty} \lambda_{v_{ym}}(t)q^m
\end{aligned} \tag{4.31}$$

$$\begin{aligned}
L[R_m(t) - \chi_m R_{m-1}(t)] &= c_o H_a \delta_{m-1}(N_1[t, \phi(t;q)]) \\
L[h_m(t) - \chi_m h_{m-1}(t)] &= c_o H_a \delta_{m-1}(N_2[t, \phi(t;q)]) \\
L[v_{xm}(t) - \chi_m v_{xm-1}(t)] &= c_o H_a \delta_{m-1}(N_3[t, \phi(t;q)]) \\
L[v_{ym}(t) - \chi_m v_{ym-1}(t)] &= c_o H_a \delta_{m-1}(N_4[t, \phi(t;q)]) \\
L[\lambda_{R_m}(t) - \chi_m \lambda_{R_{m-1}}(t)] &= c_o H_a \delta_{m-1}(N_5[t, \phi(t;q)]) \\
L[\lambda_{h_m}(t) - \chi_m \lambda_{h_{m-1}}(t)] &= c_o H_a \delta_{m-1}(N_6[t, \phi(t;q)]) \\
L[\lambda_{v_{xm}}(t) - \chi_m \lambda_{v_{xm-1}}(t)] &= c_o H_a \delta_{m-1}(N_7[t, \phi(t;q)]) \\
L[\lambda_{v_{ym}}(t) - \chi_m \lambda_{v_{ym-1}}(t)] &= c_o H_a \delta_{m-1}(N_8[t, \phi(t;q)])
\end{aligned} \tag{4.32}$$

subject to the boundary conditions,

$$\begin{aligned} R_m(0) = 0,\, h_m(0) = 0,\, v_{x_m}(0) = 0,\, v_{y_m}(0) = 0 \\ \lambda_{R_m}(0) = 0,\, \lambda_{h_m}(0) = 0,\, \lambda_{v_{x_m}}(0) = 0,\, \lambda_{v_{y_m}}(0) = 0 \end{aligned} \tag{4.33}$$

Following the approach used in Section 4.1.1, we substitute the Homotopy-Maclaurin series (Eq. (4.31)) for the states and costates to the governing equations and simplify to obtain Eq. (4.34), where $q \in [0, 1]$, and the right hand side of the Eq. (4.32) can be obtained by applying the properties of the homotopy derivative operator to the Eq. (4.34) as shown by Eq. (4.35).

$$\begin{aligned} N_1 : \dot{\phi}_R - \phi_{v_x} &= 0 \\ N_2 : \dot{\phi}_h - \phi_{v_y} &= 0 \\ N_3 : \dot{\phi_{v_x}}\sqrt{\psi^2_{\lambda_{v_x}} + \psi^2_{\lambda_{v_y}}} + \frac{F}{m}\phi_{\lambda_{v_x}} &= 0 \\ N_4 : \dot{\phi_{v_y}}\sqrt{\psi^2_{\lambda_{v_x}} + \psi^2_{\lambda_{v_y}}} + \frac{F}{m}\phi_{\lambda_{v_y}}\sqrt{\psi^2_{\lambda_{v_x}} + \psi^2_{\lambda_{v_y}}} + g\sqrt{\psi^2_{\lambda_{v_x}} + \psi^2_{\lambda_{v_y}}} &= 0 \\ N_5 : \dot{\psi_{\lambda_R}} &= 0 \\ N_6 : \dot{\psi_{\lambda_h}} &= 0 \\ N_7 : \dot{\psi_{\lambda_{v_x}}} + \psi_{\lambda_R} &= 0 \\ N_8 : \dot{\psi_{\lambda_{v_y}}} + \psi_{\lambda_h} &= 0 \end{aligned} \tag{4.34}$$

$$\begin{aligned} \delta_{m-1}(N_1) &= \dot{R}_{m-1} - v_{x_{m-1}} \\ \delta_{m-1}(N_2) &= \dot{h}_{m-1} - v_{y_{m-1}} \\ \delta_{m-1}(N_3) &= \delta_{m-1}\left(\dot{\phi_{v_x}}\sqrt{\psi^2_{\lambda_{v_x}} + \psi^2_{\lambda_{v_y}}}\right) + \frac{F}{m}\lambda_{v_{x_{m-1}}} \\ \delta_{m-1}(N_4) &= \delta_{m-1}\left(\dot{\phi_{v_y}}\sqrt{\psi^2_{\lambda_{v_x}} + \psi^2_{\lambda_{v_y}}}\right) + \frac{F}{m}\lambda_{v_{y_{m-1}}} + g\delta_{m-1}\left(\sqrt{\psi^2_{\lambda_{v_x}} + \psi^2_{\lambda_{v_y}}}\right) \\ \delta_{m-1}(N_5) &= \dot{\lambda}_{R_{m-1}} \\ \delta_{m-1}(N_6) &= \dot{\lambda}_{h_{m-1}} \\ \delta_{m-1}(N_7) &= \dot{\lambda}_{v_{x_{m-1}}} + \lambda_{R_{m-1}} \\ \delta_{m-1}(N_8) &= \dot{\lambda}_{v_{y_{m-1}}} + \lambda_{h_{m-1}} \end{aligned} \tag{4.35}$$

4.2.2 Selection of Initial Guess, Linear Operator, and Auxiliary Function (Classical 2D Ascent Problem)

The choice of the basis functions and the *rule of solution expression* is the same as used for the simple control problem given by Eq. (3.40). A same approach is used for the selection of initial guess as used in the previous problems. Only the initial boundary conditions are used to build the initial guess. Eq. (4.36) gives the set of equations for the initial guesses of each state and costate.

$$\begin{aligned}
R_0(t) &= \sum_{m=0}^{1} b_{1m} e_m(t) = b_{11} e_1 + b_{12} e_2 \\
h_0(t) &= \sum_{m=0}^{1} b_{2m} e_m(t) = b_{21} e_1 + b_{22} e_2 \\
v_{x_0}(t) &= \sum_{m=0}^{1} b_{3m} e_m(t) = b_{31} e_1 + b_{32} e_2 \\
v_{y_0}(t) &= \sum_{m=0}^{1} b_{4m} e_m(t) = b_{41} e_1 + b_{42} e_2 \\
\lambda_{R_0}(t) &= \sum_{m=0}^{1} b_{5m} e_m(t) = b_{51} e_1 + b_{52} e_2 \\
\lambda_{h_0}(t) &= \sum_{m=0}^{1} b_{6m} e_m(t) = b_{61} e_1 + b_{62} e_2 \\
\lambda_{v_{x_0}}(t) &= \sum_{m=0}^{1} b_{7m} e_m(t) = b_{71} e_1 + b_{72} e_2 \\
\lambda_{v_{y_0}}(t) &= \sum_{m=0}^{1} b_{8m} e_m(t) = b_{81} e_1 + b_{82} e_2
\end{aligned} \tag{4.36}$$

where e_m is given by Eq. (3.39). From Table 4.5, it can be seen that the initial conditions for the costates are not provided. Hence, we can select unknown parameters for those values. We are also required to find the optimal final time for this case, which gives us t_f as the fifth unknown parameter to be calculated. The values of the coefficients chosen to build the initial guess are given in Table 4.6

A same approach for the selection of linear operator and auxiliary function are used as described in the Section 3.2.3. The value of K_1 is chosen to be 1, since the

Table 4.6: Coefficients and initial guess - classical 2D ascent problem.

j	state and costate	Coefficient b_{j1}	Coefficient b_{j2}	Initial Guess
1	R	0	0	0
2	h	0	0	0
3	v_x	0	0	0
4	v_y	0	0	0
5	λ_R	0	β_1	β_1
6	λ_h	0	β_2	β_2
7	λ_{v_x}	0	β_3	β_3
8	λ_{v_y}	0	β_4	β_4

highest order of derivative for all the governing equations is 1. Using Eq. (4.18), we obtain the linear operator as $\frac{d}{dt}$. The auxiliary function is selected to be 1 by using a same approach as in section 4.1.2. Using Eqs. (4.32) and (4.35), we write the m^{th} order deformation equations given by Eq. (4.37), where, χ_m is given by Eq. (3.16). All the constants of integration are calculated using the boundary conditions in Eq. (4.33).

$$
\begin{aligned}
R_m(t;c_o) &= \chi_m R_{m-1}(t) + c_o \int_0^t (\dot{R}_{m-1} - v_{x_{m-1}})dt + C_1 \\
h_m(t;c_o) &= \chi_m h_{m-1}(t) + c_o \int_0^t (\dot{h}_{m-1} - v_{y_{m-1}})dt + C_2 \\
v_{x_m}(t,c_o) &= \chi_m v_{x_{m-1}}(t) + c_o \int_0^t \left[\delta_{m-1}\left(\dot{\phi_{v_x}}\sqrt{\psi^2_{\lambda_{v_x}} + \psi^2_{\lambda_{v_y}}}\right) + \frac{F}{m}\lambda_{v_{x_{m-1}}}\right]dt + C_3 \\
v_{y_m}(t,c_o) &= \chi_m v_{y_{m-1}}(t) + c_o \int_0^t \left[\delta_{m-1}\left(\dot{\phi_{v_y}}\sqrt{\psi^2_{\lambda_{v_x}} + \psi^2_{\lambda_{v_y}}}\right) + \frac{F}{m}\lambda_{v_{y_{m-1}}} + \right. \\
&\qquad \left. g\delta_{m-1}\left(\sqrt{\psi^2_{\lambda_{v_x}} + \psi^2_{\lambda_{v_y}}}\right)\right]dt + C_4 \\
\lambda_{R_m}(t;c_o) &= \chi_m \lambda_{R_{m-1}}(t) + c_o \int_0^t (\dot{\lambda}_{R_{m-1}})dt + C_5 \\
\lambda_{h_m}(t;c_o) &= \chi_m \lambda_{h_{m-1}}(t) + c_o \int_0^t (\dot{\lambda}_{h_{m-1}})dt + C_6 \\
\lambda_{v_{x_m}}(t;c_o) &= \chi_m \lambda_{v_{x_{m-1}}}(t) + c_o \int_0^t (\dot{\lambda}_{v_{x_{m-1}}} + \lambda_{R_{m-1}})dt + C_7 \\
\lambda_{v_{y_m}}(t;c_o) &= \chi_m \lambda_{v_{y_{m-1}}}(t) + c_o \int_0^t (\dot{\lambda}_{v_{y_{m-1}}} + \lambda_{h_{m-1}})dt + C_8
\end{aligned}
\tag{4.37}
$$

4.2.3 Results (Classical 2D Ascent Problem)

Using the same approach as discussed previously, we assume $c_o = -1$. The 5 terminal boundary conditions on the states, costates, and final time allows us to build a non-linear system of equations in β_1, β_2, β_3, β_4, and t_f. 1^{st} order series solutions are found to be trivial and are unable to capture the non-linearity of the problem. Therefore, in this problem, we begin with calculating 2^{nd} order series solutions. Using the previous approach, we use the parameter values obtained for the 2^{nd} order solution as the initial guess for the 3^{rd} order solution input to Fsolve. Table 4.7 provides the initial guesses for the 2^{nd} order solution and the values obtained for the consecutive orders series solutions using Fsolve. It can be observed that for higher order solutions, the parameter values have started to converge, but the convergence process is slow.

Table 4.7: Parameter values - classical 2D ascent problem.

Order of solution	β_1	β_2	β_3	β_4	$t_f[s]$
Initial guess for 2^{nd} order	0.1	0.1	0.1	0.1	800
2	1.1554×10^{-27}	-0.0005	0.2450	0.2242	819.1950
3	-2.0175×10^{-34}	-0.0006	-0.1721	-0.2463	806.5123
4	-1.2741×10^{-31}	-0.0006	-0.1541	-0.2388	719.0774
5	1.1392×10^{-32}	-0.0006	-0.1391	-0.2353	670.8889
6	-6.7729×10^{-32}	-0.0006	-0.1295	-0.2309	633.3053
7	-6.5394×10^{-31}	-0.0006	-0.1226	-0.2278	604.9100
8	3.8722×10^{-31}	-0.0006	-0.1176	-0.2258	582.5482
9	2.1616×10^{-34}	-0.0006	-0.1139	-0.2253	564.5248
10	2.4196×10^{-31}	-0.0006	-0.1114	-0.2262	549.6620
11	5.1269×10^{-32}	-0.0006	-0.1100	-0.2290	537.1408
11^{th} order for optimal c_o	-1.5020×10^{-29}	-0.0006	-0.1088	-0.2280	519.7829

Fig. 4.8 shows the c_o curves for the domain $c_o \in [-2, 0]$ for the 11^{th} order series solutions. It can be concluded that no common horizontal range can be identified for

which any of the physical quantities converge. Therefore, it is not possible to apply convergence a control to this problem.

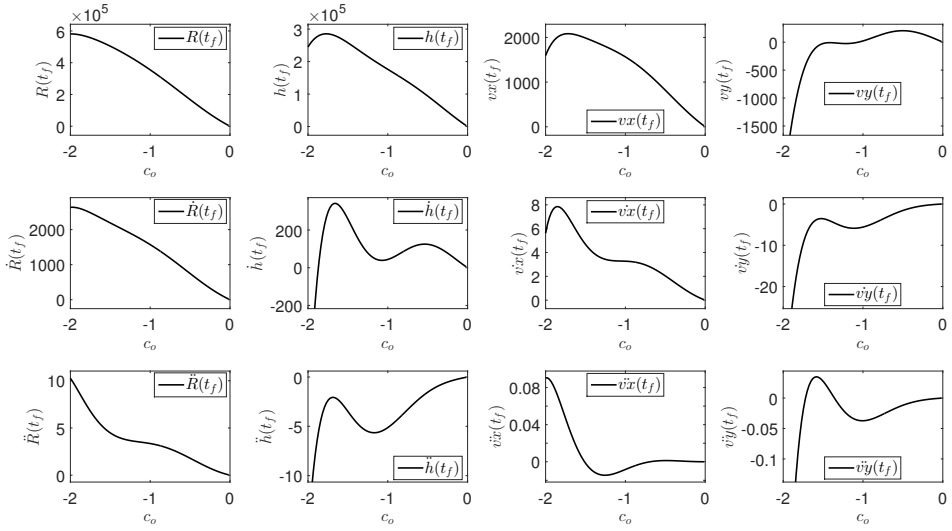

Figure 4.8.: $c_o \sim$ curves for $c_o \in [-2, 0]$ - classical 2D ascent problem.

The optimal c_o of -1.0594 is calculated for the 11^{th} order solution by minimizing the total squared discrete residual over the c_o range, $[-10^{10}, 10^{10}]$. The values of the parameters are recalculated for the optimal c_o and are provided in the last row of Table 4.7. Figs. 4.9 and 4.10 provide a comparison of the state and costate trajectories for the 11^{th} order series solutions with those obtained from *bvp4c*.

Fig. 4.11 shows the comparison of the control histories from the two methods. It can be seen from Fig. 4.12(a), that compared to the 2^{nd} order solution, the total discrete squared residual reduces by almost 3 orders for the 11^{th} order solution. Using the optimal c_o, the total discrete squared residual reduces to 901.06 from 1216.73 for the 11^{th} order series solution. Fig. 4.12(b) shows the exponential increase in CPU-time for higher orders of solution. The time recorded for the 11^{th} order solution (10175 s) is almost quadruple that of that required by the 10^{th} order solution (2544 s). Due to these high computation times, it was decided to truncate the solution at the 11^{th} order.

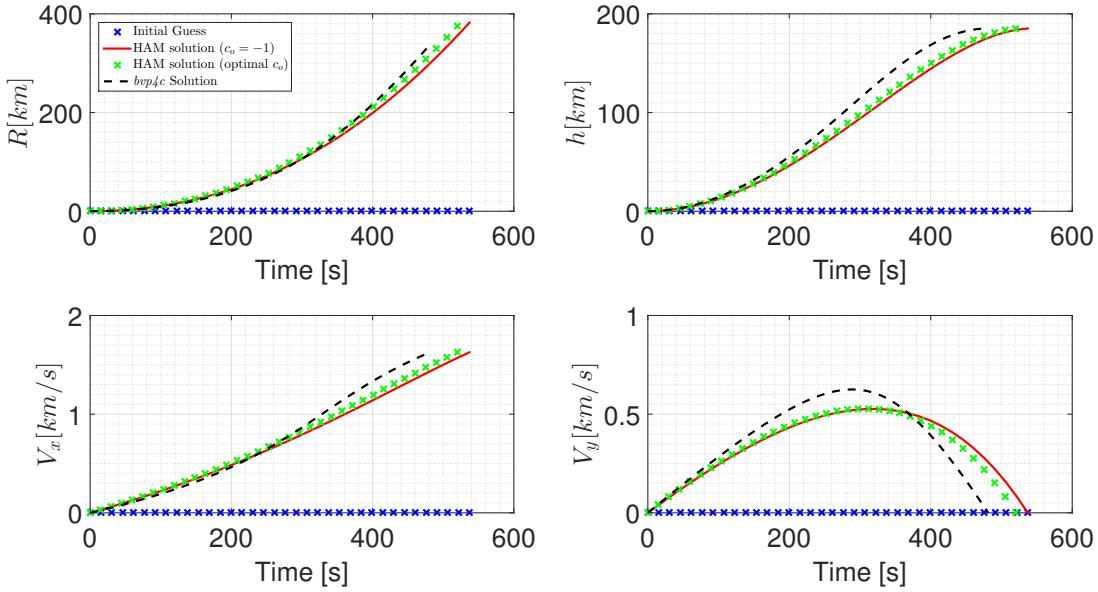

Figure 4.9.: States from 11^{th} order HAM solution - classical 2D ascent problem.

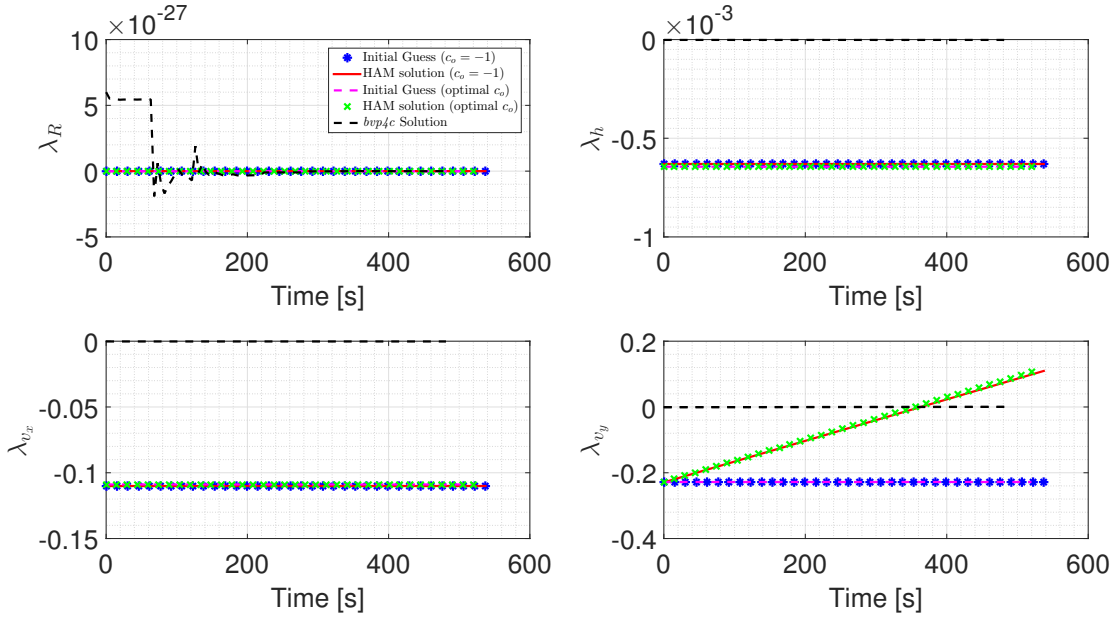

Figure 4.10.: Costates from 11^{th} order HAM solution - classical 2D ascent problem.

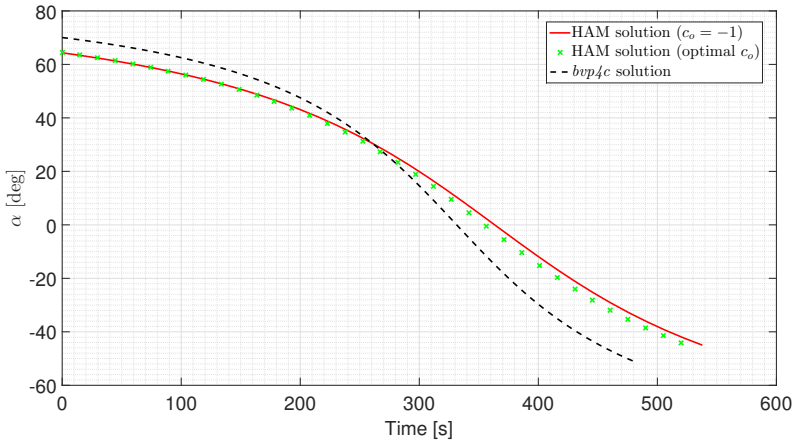

Figure 4.11.: Control history - classical 2D ascent problem.

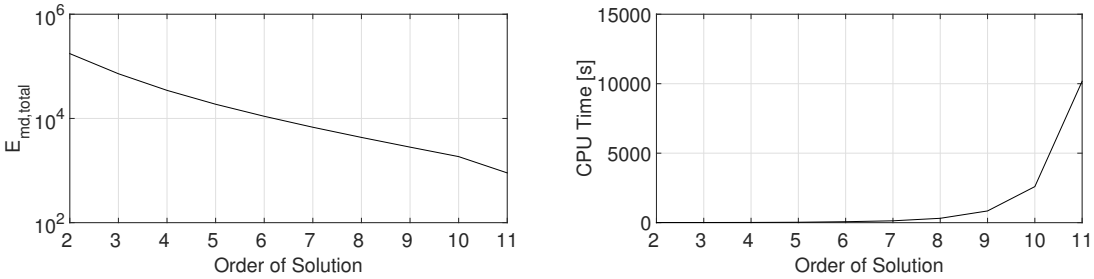

(a) $E_{md,Total}$ vs order of solution

(b) CPU time vs order of solution

Figure 4.12.: Computational performance - classical 2D ascent problem.

4.3 2D Ascent Launch Problem (Fixed Final-Time Problem)

For the second test case, the 2D ascent problem was modified to a fixed final-time problem. A vehicle launched from the surface of the Earth must reach an orbit of 185.2 km in 485 seconds to achieve a maximum terminal horizontal component of velocity. The assumptions for this case are the following:

1. An instantaneous steering angle α is the only control variable.
2. The acceleration due to gravity from the Earth is assumed to be 9.8 m/s^2.
3. Thrust to weight ratio for the vehicle is 3.

4. A constant mass and a constant thrust force F is assumed.

5. Final altitude to be achieved is 185.2 km.

6. There is no atmosphere and no aerodynamic forces on the vehicle.

The objective function for this case is defined by Eq. (4.38)

$$\text{Min } J = \ -v_{x_f} \tag{4.38}$$

with the dynamics given by Eq. (4.21), where g = 9.8 m/s^2. The acceleration is calculated using Eq. (4.39)

$$\frac{F}{m} = (\text{Thrust to weight})(g) = 29.4\,\text{m/s}^2 \tag{4.39}$$

The expression for the Hamiltonian and the dynamics for costates are the same as used in the previous case given by the Eqs. (4.23) and (4.24), respectively. Using Pontryagin's Minimum Principle, we obtain the control law given by Eq. (4.25) and the state equations by Eq. (4.30). We use the transversality condition to obtain two additional terminal boundary conditions on the costates λ_R and λ_{v_x}. The boundary conditions for the fixed final-time problem are given in Table. 4.8.

4.3.1 HAM Formulation (Fixed Final-Time Problem)

As the classical ascent problem is modified, Eqs. (4.31) - (4.37) also describe the HAM problem formulation for the fixed final time problem as well. The same initial guess (Table 4.6), linear operator, and auxiliary function as for the classical ascent case are also used for this case. The final time is provided in this problem, so there is no need to define the parameter, t_f, for this case. The 4 terminal boundary conditions given in Table. 4.8 are used to build a nonlinear system of equations in the 4 unknown parameters β_1, β_2, β_3 and β_4. Table 4.9 lists the values of parameters obtained at each order of solution. It is clear that, at higher orders of solutions, the values do not differ by much. The optimal c_o is calculated to be -1.0001.

Table 4.8: Boundary conditions - 2D ascent fixed final-time problem.

state and costate	Initial condition	Terminal condition
R	0 km	free
h	0 km	185.2 km
v_x	0 m/s	free
v_y	0 m/s	0 m/s
λ_R	free	0
λ_h	free	free
λ_{vx}	free	-1
λ_{vy}	free	free

Table 4.9: Parameter values - 2D ascent fixed final-time problem

Order of solution	β_1	β_2	β_3	β_4
Initial guess for 2^{nd} order	0.1	0.1	0.1	0.1
2	0	-0.0002	-1	-0.4143
3	0.0008	-0.0006	-0.9999	-0.5974
4	3.1245×10^{-30}	-0.0006	-1	-0.5133
5	0.0001	-0.0011	-0.9999	-0.6330
6	-1.2526×10^{-31}	-0.0007	-1	-0.5422
7	-7.0779×10^{-30}	-0.0008	-1	-0.5611
8	4.7335×10^{-27}	-0.0007	-1	-0.5500
9	-1.1268×10^{-26}	-0.0008	-1	-0.5547
10	2.1571×10^{-30}	-0.0007	-1	-0.5522
11	1.3146×10^{-28}	-0.0008	-1	-0.5534
11^{th} order for optimal c_o	-2.4329×10^{-29}	-0.0008	-1	-0.5533

4.3.2 Results (Fixed Final-Time Problem)

Fig. 4.13 shows the c_o curves for the 11^{th} order series solutions. Similar to the previous case, no common horizontal region can be found out for which all the physical quantity converge. We use the same approach and use the optimal c_o for calculating the series solutions. Figs. 4.14 and 4.15 depict the series solution with the *bvp4c* solution. Fig. 4.16 shows the comparison between the control histories obtained from HAM and *bvp4c* methods. Due to the accurate solutions obtained for both states and costates, the control profiles are in good agreement. Figs. 4.17(a) and 4.17(b) show the total discrete squared residual and CPU-time for the fixed final-time problem.

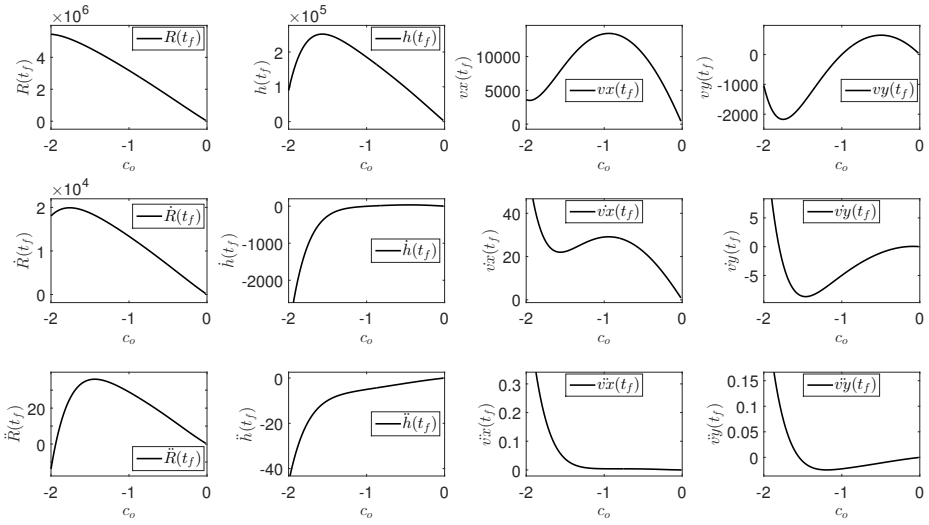

Figure 4.13.: $c_o \sim$ curves for $c_o \in [-2, 0]$ - 2D ascent fixed final-time problem.

On comparison of the two ascent cases from Table 4.7 and Table 4.9, it can be concluded that the presence of an extra parameter, t_f in the non-linear system led to slow convergence rate of the first case. It was also found that the non-linear system formulated is sensitive to initial guess provided to Fsolve function. Using a negative value for the final-time parameter t_f, resulted in non-physical results.

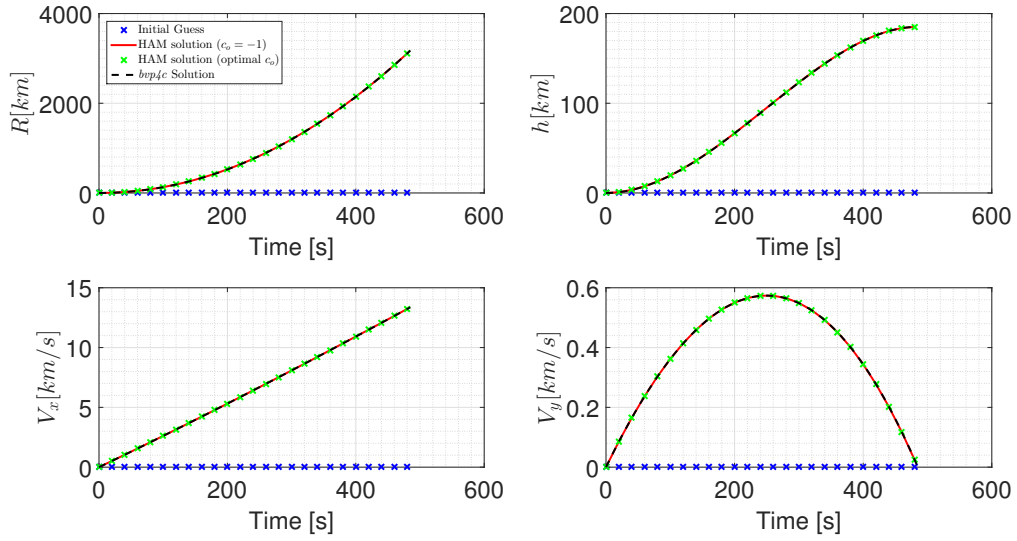

Figure 4.14.: States from 11^{th} order HAM solution - 2D ascent fixed final-time problem.

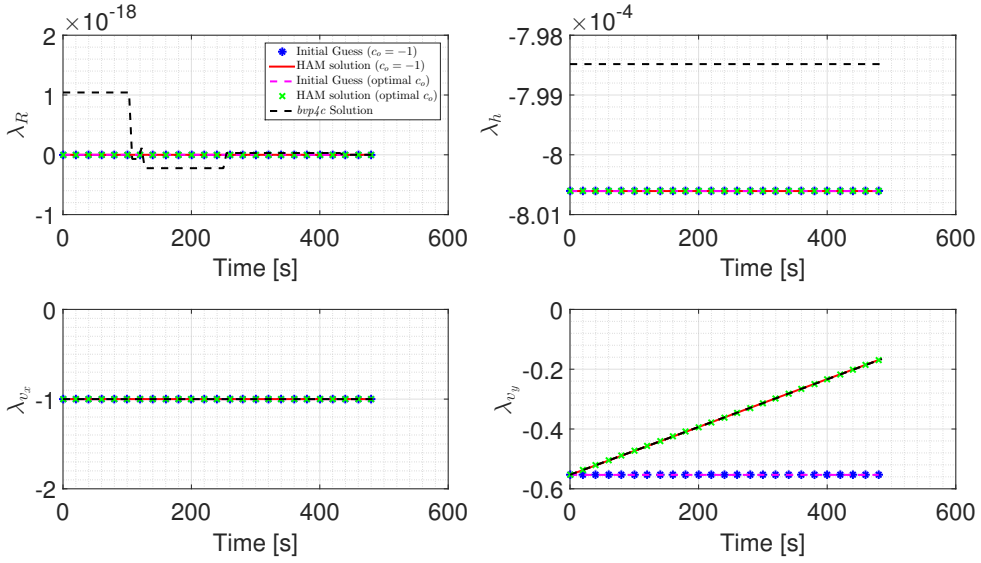

Figure 4.15.: Costates from 11^{th} order HAM solution - 2D ascent fixed final-time problem.

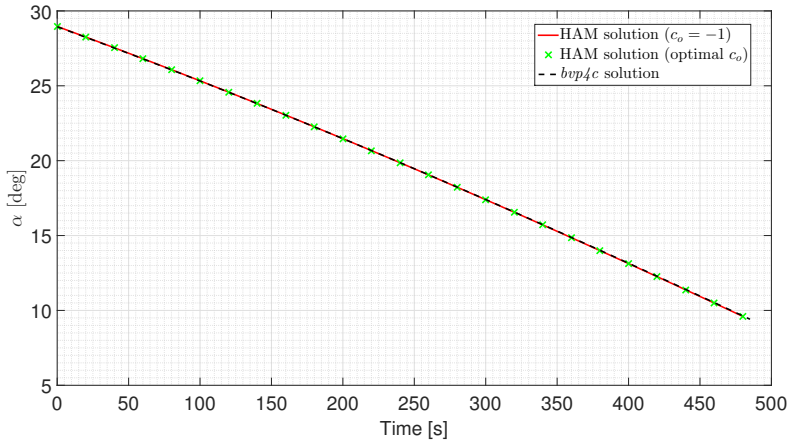

Figure 4.16.: Control history - 2D ascent fixed final-time problem.

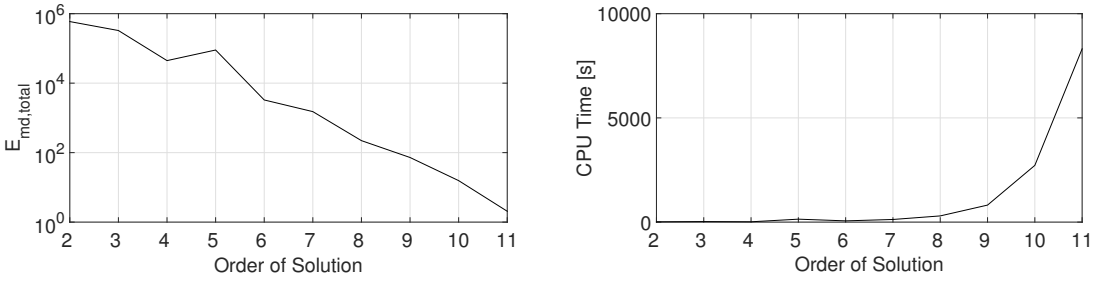

(a) $E_{md,Total}$ vs order of solution

(b) CPU time vs order of solution

Figure 4.17.: Computational performance - 2D ascent free final-time problem.

Table. 4.10 compares the total discrete squared residual and CPU-time for the two ascent cases at 11^{th} order solution. The lower total discrete squared residual and low CPU-time for the latter case can be justified by solving for 4 parameters instead of 5 in the previous case. A 6^{th} order HAM solution for the ascent problem results in a non-linear system consisting of equations with as many as 1730 analytical terms.

The modified fixed final-time ascent case was also tried for the Moon. Following the same approach as used in the previous ascent cases, a new non-linear system was generated by using the Gravitational constant for the Moon. The initial guess for Fsolve was provided using the same approach as described for the ascent cases.

Table 4.10: Comparison of computational performance for two ascent cases (11^{th} order solution).

Test-case	$E_{md,Total}$	CPU-time [s]
Free final-time (Moon)	901.06	10175
Fixed final-time (Earth)	2.03	8419

However, as compared to the previous cases, the convergence of parameter values was not obtained. Based on this observation, there could be a possibility that simply changing the value of the Gravitational constant resulted in an ill-conditioned system. To investigate this fact, scaling of the dynamics can be performed prior to solving the non-linear system. It can be concluded that convergence for HAM based approach depends highly on the intermediate step of solving the non-linear system. Since this step employs Fsolve, which depends on the initial guess provided, there is a need of search for more robust numerical solvers for large non-linear system of equations.

It should be noted that the current HAM based approach uses initial guesses based on only the initial boundary conditions for the state and costate variables. An initial framework for solving indirect trajectory optimization has been built, and a working example of an aerospace application shows the possibility that the approach can be used to replace the difficult practices used for building initial guesses.

5. SUMMARY

This study shows use of the Homotopy Analysis Method to solve trajectory optimization problems using the indirect approach. The approach is tested on several optimal control problems, and specific challenges are discovered in the process. The boundary value problems generated using the necessary conditions of optimality are solved using HAM to generate approximate analytical series solutions for the state, costate, and control variables.

The boundary value problem is converted into an initial value problem by assigning the unknown initial conditions as parameters. Using symbolic computations, the HAM approach generates analytical series expressions for state and costate variables in terms of the parameters and the convergence control parameter, c_o. A non-linear system of equations is generated by assuming the value of c_o to be -1. The non-linear equations are solved numerically for each order to generate the values for the parameters. c_o ∼curves are plotted for physical quantities like $x(t_f) \sim c_o$, $\dot{x}(t_f) \sim c_o$ and $\ddot{x}(t_f) \sim c_o$ to check for horizontal regions, which depict convergence domains. c_o can be adjusted to lie in the common convergence domain of the all the physical quantities corresponding to all the state and costate variables. An optimal c_o can be calculated for that range by minimizing the total discrete squared residual, a measure of how well the series solutions satisfy the dynamics. Using the optimal c_o, this process is repeated to calculate the parameters and the adjusted results show an improvement in the accuracy of the solution.

The process is demonstrated to solve Zermelo's problem and two test cases of the 2D ascent problem. The convergence properties of various physical quantities for the states and costates do not allow for the convergence control process, but the optimal value of c_o is close to -1. The solution for the free final-time case of the 2D ascent problem is found to be more difficult to converge to as compared to the fixed final-

time case. Due to the presence of an extra parameter, t_f, in the non-linear system to be solved, the convergence slows down, and the solutions have to be truncated due to a high computational cost. The 11^{th} order series solutions for both test cases show a major difference in accuracy on comparison of the total discrete squared residual. The current HAM based approach suffers from unreliability in convergence of the numerical solution for the non-linear system generated. The approach currently employs the use of MATLAB's Fsolve function to solve the non-linear system, which depends highly on the initial guess provided. This was concluded due to the failure to obtain convergence for the 2D ascent fixed final-time Moon problem.

The high computational cost and lower accuracy of the solutions are compensated by the ease and convenience of the problem formulation. Two of the major challenges for conventional indirect methods - the initial guess generation and small domain of convergence can be addressed using a well-defined approach in HAM. The possibility of finding a convergence region for a trajectory optimization problem gives more insight into the problem and can be very beneficial.

6. FUTURE WORK

6.1 Using Tolerances for Stopping Criteria

As explained in Section 3.6, the HAM process for an indirect trajectory optimization problem is terminated by the designer by visual comparison of the results with the *bvp4c* solver. This step can be automated by comparing the values of the discrete squared residual for each governing equation at all orders of the solution, with a tolerance defined by the designer. Another metric based on the difference between the discrete squared residual for two consecutive orders of the solution will give an insight into the improvement with an increase in order. Terminal boundary conditions can also be compared with a defined tolerance. If any of the metrics do not satisfy the stopping criteria, then the process will continue to solve for higher orders of the solution. This is depicted by the flowchart in Fig. 6.1 .

6.2 Parallelizing HAM

High performance computing architectures are moving towards parallel systems based on single-node, multiple-core systems. The basic requirement for a problem to be parallelized is the possibility of dividing it into several smaller independent problems. While implementing the HAM approach to boundary value problems, it has been found that of all the steps used, the maximum computational resources are required to obtain the m^{th} order deformation equations. These equations are derived by integrating large symbolic expressions in multiple variables. Each of the consecutive deformation equations for a state variable contains terms from the previous order deformation equations for multiple variables. This results in recurring terms as shown in the Section 3.1.1. At the m^{th} order, the deformation equation for a variable de-

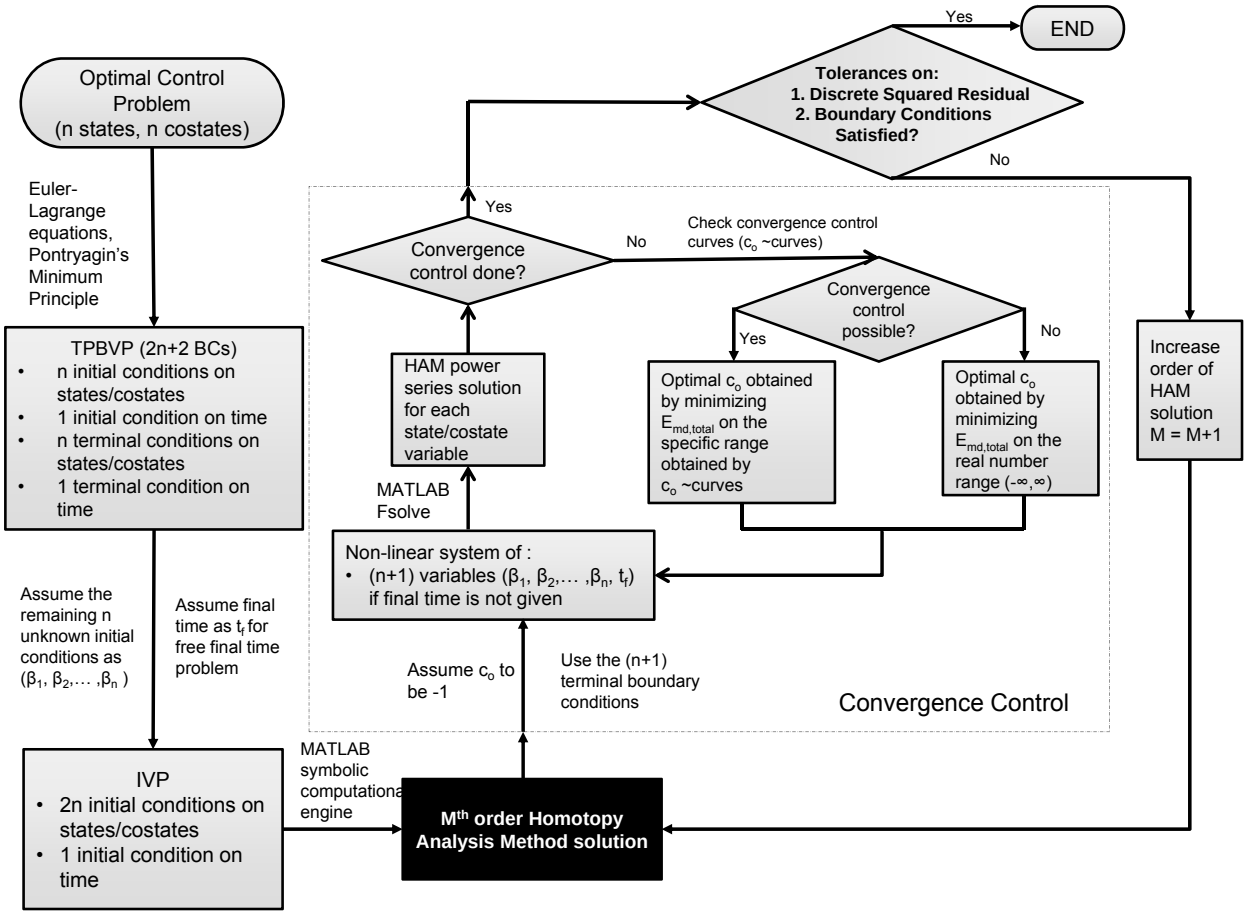

Figure 6.1.: Updated flowchart for the HAM process.

pends only on the terms from the $(m-1)^{th}$ order solution and is independently solved for each state and co-state variable. This fact makes the HAM approach capable of being parallelized. For a problem consisting of n state and co-state variables, the computation time can be reduced by a factor of 2n for each order of solution.

6.3 Implementing Recurrence Formulae

The authors of Ref. [47, 61] used an approach to obtain the higher order terms of the series solution without integrating the m^{th} order deformation equations for higher orders. Since, all the state and co-state variables are calculated to be series solutions in the independent variable, they can directly be represented as Eq. (6.1) for the simple control problem

$$\begin{aligned} x_m(t, c_o) &= \sum_{n=0}^{m} x_{m,n} t^n \\ \lambda_m(t, c_o) &= \sum_{n=0}^{m} \lambda_{m,n} t^n \end{aligned} \tag{6.1}$$

These series expressions can directly be substituted into the m^{th} order deformation Eq. (3.45). On the right hand side of the equation, the terms with common powers of t are collected and the coefficients are compared with the terms on the left hand side of the equation. Observing the coefficients obtained from the first few orders of solutions, recurrence formulae can be build for $x_{m,n}$ and $\lambda_{m,n}$. The major challenge in this approach arises with manually finding the patterns for the first few order solutions. Since the dynamics for trajectory optimization problems are highly non-linear, the resulting first few terms are embedded with multiple unknown parameters (β_1, β_2, β_3, t_f) and c_o, which makes the process of finding recurrence patterns extremely difficult.

6.4 Hybrid Methods

Due to good convergence properties and analytical nature of the solution, HAM is susceptible to less number of numerical failures and singularities as compared to the conventional indirect trajectory optimization methods. One possible approach to reduce the uncertainty in convergence of indirect methods is to merge the HAM method with conventional indirect methods. The good convergence properties of HAM can be utilized to produce high quality initial guesses to seed the multiple shooting method. Since HAM is computationally intensive, lower order solutions are expected to be within the small convergence region of the shooting methods.

LIST OF REFERENCES

LIST OF REFERENCES

[1] Albert L. Herman and Bruce A. Conway. Direct optimization using collocation based on high-order gauss-lobatto quadrature rules. *Journal of Guidance, Control, and Dynamics*, 19(3):592–599, 1996.

[2] Robert Bibeau and D. Rubenstein. Trajectory optimization for a fixed-trim reentry vehicle using direct collocation and nonlinear programming. In *AIAA Guidance, Navigation, and Control Conference and Exhibit*, 2000.

[3] J. Betts. *Practical Methods for Optimal Control and Estimation Using Nonlinear Programming*. Society for Industrial and Applied Mathematics, second edition, 2010.

[4] Michael J. Grant and Robert D. Braun. Rapid indirect trajectory optimization for conceptual design of hypersonic missions. *Journal of Spacecrafts and Rockets*, 52(1), 2015.

[5] I. Michael Ross. A beginners guide to dido. Technical report, Ellisar, LLC, Monterey, CA, 2007.

[6] Michael A. Patterson and Anil V. Rao. Gpops-ii: A matlab software for solving multiple-phase optimal control problems using hp-adaptive gaussian quadrature collocation methods and sparse nonlinear programming. *ACM Trans. Math. Softw.*, 41(1):1:1–1:37, October 2014.

[7] Fariba Fahroo and I. Michael Ross. Costate estimation by a legendre pseudospectral method. *Journal of Guidance, Control, and Dynamics*, 24(2):270–277, 2001.

[8] Charles R. Hargraves and Stepehn W. Paris Adams. Direct trajectory optimization using nonlinear programming and collocation. *Journal of Guidance, Control, and Dynamics*, 10(4):338–342, 1987.

[9] Philip E. Gill, Walter Murray, and Michael A. Saunders. Snopt: An sqp algorithm for large-scale constrained optimization. *SIAM Review*, 47(1):99–131, 2005.

[10] Lev D. Elsgolc. *Calculus of Variations*. Dover, New York, 2007.

[11] Revaz V. Gamkrelidze Vladimir G. Boltyanskii and Lev S. Pontryagin. Towards a theory of optimal processes. *Proceedings of the USSR Academy of Sciences*, 110(1):7–10, 1956.

[12] Joseph Stoer and R. Bulirsch. *Introduction to Numerical Analysis*. Springer, New York, 3 edition, 2002.

[13] O. von Stryk and R. Bulirsch. Direct and indirect methods for trajectory optimization. *Annals of operation research*, 37(1):357–373, 1992.

[14] R. Bulirsch K. Chudej and K.D. Reinsch. Optimal ascent and staging of a two-stage space vehicle system. *DGLR 1*, pages 243–293, 1990.

[15] Martin Hermann and Masoud Saravi. *Nonlinear ordinary differential equations-Analytical approximation and numerical methods*. Springer, India, 2016.

[16] Ji-Huan He. Variational iteration method a kind of non-linear analytical technique: some examples. *International Journal of Non-Linear Mechanics*, 34:699–708, 1999.

[17] G. Adomian. *Solving Frontier Problems of Physics: The Decomposition Method*. Springer, georgia, USA, 1994.

[18] A.M. Lyapunov. *The general problem of the stability of motion*. Taylor and Francis, London, 1992.

[19] V.G. Kolosov A.V. Karmishin, A.T. Zhukov. Methods of dynamics calculation and testing for thin-walled structures (in russian). 1990.

[20] M. Van Dyke. *Perturbation methods in fluid mechanics*. Academic Press, London, 1964.

[21] Shijun Liao. *Homotopy Analysis Method in Nonlinear Differential Equations*. Higher Education Press, Beijing, China, 2012.

[22] Shijun Liao. *The proposed homotopy analysis technique for the solution of nonlinear problems*. PhD thesis, Shanghai Jiao Tong University, Shanghai, China, 1992.

[23] Shijun Liao. *Beyond Perturbation: Introduction to Homotopy Analysis Method*, chapter 2, pages 17–31. Chapman & Hall, Florida, USA, 2004.

[24] Shijun Liao. *Beyond Perturbation: Introduction to Homotopy Analysis Method*, chapter 4, pages 76–85. Chapman & Hall, Florida, USA, 2004.

[25] Ji-Huan He. Homotopy perturbation technique. *Computer Methods in Applied Mechanics and Engineering*, 178(3):257–262, 1999.

[26] Shijun Liao. *Homotopy Analysis Method in Nonlinear Differential Equations*, chapter 4, pages 143–197. Higher Education Press, Beijing, China, 2012.

[27] A.E. Bryson and Y.C. Ho. *Applied Optimal Control Optimization, Estimation, and Control*. Taylor & Francis, 1975.

[28] David D. Morrison, James D. Riley, and John F. Zancanaro. Multiple shooting method for two-point boundary value problems. *Commun. ACM*, 5(12):613–614, December 1962.

[29] Jacek Kierzenka and Lawrence F. Shampine. A bvp solver based on residual control and the matlab pse. *ACM Transactions on Mathematical Software*, 27(3):299–316, 2001.

[30] J. C. Alexander and James A. Yorke. The homotopy continuation method: numerically implementable topological procedures. *Trans. Amer. Math. Soc.*, 242:271–284, 1978.

[31] P. Deuflhard H.J. Pesch and P. Rentrop. A modified continuation method for the numerical solution of nonlinear two-point boundary value problems by shooting techniques. *Numer. Math.*, 26:327–343, 1976.

[32] Knut Graichen and Nicolas Petit. A continuation approach to state and adjoint calculation in optimal control applied to the reentry problem. *IFAC Proceedings Volumes*, 41(2):1430714312, 2008.

[33] Joseph Gergaud and Thomas Haberkorn. Homotopy method for minimum consumption orbit transfer problem. *ESAIM: Control, Optimisation and Calculus of Variations*, 12(2):294–310, 2006.

[34] Y. Gao and C. A. Kluever. Low-thrust interplanetary orbit transfers using hybrid trajectory optimization method with multiple shooting. In *AIAA/AAS Astrodynamics Specialist Conference and Exhibit*, page 213, Providence, Rhode Island, 2004.

[35] Peter Friedrich Gath. *CAMTOS - A Software Suite Combining Direct and Indirect Trajectory Optimization Methods*. PhD thesis, Institut fr Flugmechanik und Flugregelung, University of Stuttgart, Germany, 11 2002.

[36] Shijun Liao. A new branch of solutions of boundary-layer flows over an impermeable stretched plate. *International Journal of Heat and Mass Transfer*, 48(12):2529 – 2539, 2005.

[37] Shijun Liao. A uniformly valid analytic solution of two-dimensional viscous flow over a semi-infinite flat plate. *Journal of Fluid Mechanics*, 385:101–128, April 1999.

[38] Shijun Liao. An explicit, totally analytic approximate solution for blasius viscous flow problems. *International Journal of Non-Linear Mechanics*, 34:759–778, 1999.

[39] Shijun Liao and Antonia Campo. Analytic solutions of the temperature distribution in blasius viscous flow problems. *Journal of Fluid Mechanics*, 453:411–425, 2 2002.

[40] Shijun Liao. On the analytic solution of magnetohydrodynamic flows of nonnewtonian fluids over a stretching sheet. *Journal of Fluid Mechanics*, 488:189–212, 7 2003.

[41] Shijun Liao. Series solutions of unsteady boundary-layer flows over a stretching flat plate. *Studies in Applied Mathematics*, 117(3):239–263, 2006.

[42] Shijun Liao. An analytic approximation of the drag coefficient for the viscous flow past a sphere. *International Journal of Non-Linear Mechanics*, 37(1):1 – 18, 2002.

[43] S Abbasbandy, E Magyari, and E Shivanian. The homotopy analysis method for multiple solutions of nonlinear boundary value problems. *Communications in Nonlinear Science and Numerical Simulation*, 14(9):3530–3536, 2009.

[44] S Abbasbandy. The application of homotopy analysis method to solve a generalized hirota–satsuma coupled kdv equation. *Physics Letters A*, 361(6):478–483, 2007.

[45] S Abbasbandy. The application of homotopy analysis method to nonlinear equations arising in heat transfer. *Physics Letters A*, 360(1):109–113, 2006.

[46] S Abbasbandy and E Shivanian. Predictor homotopy analysis method and its application to some nonlinear problems. *Communications in Nonlinear Science and Numerical Simulation*, 16(6):2456–2468, 2011.

[47] Kazuki Yabushita, Mariko Yamashita, and Kazuhiro Tsuboi. An analytic solution of projectile motion with the quadratic resistance law using the homotopy analysis method. *Journal of Physics A: Mathematical and Theoretical*, 40(29):8403, 2007.

[48] Saeid Abbasbandy and Ahmand Shirzadi. The series solution of problems in the calculus of variations via the homotopy analysis method. *A Journal of Physical Sciences*, (1), 2009.

[49] H. Saberi Nik and Stanford Shateyi. Application of optimal ham for finding feedback control of optimal control problems. *Mathematical Problems in Engineering*, 2013, 2013.

[50] Moosarreza Shamsyeh Zahedi and Hassan Saberi Nik. On homotopy analysis method applied to linear optimal control problems. *Applied Mathematical Modelling*, 37(23):9617 – 9629, 2013.

[51] H Saberi Nik, Sohrab Effati, Sandile Sydney Motsa, and Mohammad Shirazian. Spectral homotopy analysis method and its convergence for solving a class of nonlinear optimal control problems. *Numerical Algorithms*, 65(1):171–194, 2014.

[52] S Effati, H Saberi Nik, and A Jajarmi. Hyperchaos control of the hyperchaotic chen system by optimal control design. *Nonlinear Dynamics*, 73(1-2):499–508, 2013.

[53] H Saberi Nik, Sohrab Effati, Sandile S Motsa, and Stanford Shateyi. A new piecewise-spectral homotopy analysis method for solving chaotic systems of initial value problems. *Mathematical Problems in Engineering*, 2013, 2013.

[54] H Saberi Nik, Sohrab Effati, Sandile Sydney Motsa, and Mohammad Shirazian. Spectral homotopy analysis method and its convergence for solving a class of nonlinear optimal control problems. *Numerical Algorithms*, 65(1):171–194, 2014.

[55] Shijun Liao. *Beyond Perturbation: Introduction to Homotopy Analysis Method*, chapter 3, pages 61–74. Chapman & Hall, Florida, USA, 2004.

[56] Shijun Liao. *Homotopy Analysis Method in Nonlinear Differential Equations*, chapter 7, pages 239–278. Higher Education Press, Beijing, China, 2012.

[57] Shijun Liao. *Homotopy Analysis Method in Nonlinear Differential Equations*, chapter 13, pages 425–457. Higher Education Press, Beijing, China, 2012.

[58] Wolfram Research. Mathematica 8.0, 2010.

[59] Michael B. Monagan, Keith O. Geddes, K. Michael Heal, George Labahn, Stefan M. Vorkoetter, James McCarron, and Paul DeMarco. *Maple 10 Programming Guide*. Maplesoft, Waterloo ON, Canada, 2005.

[60] James M. Longuski , Jose J. Guzman and John E. Prussing. *Optimal Control with Aerospace Applications*. Springer, New York, 2014.

[61] T. Hayat and M. Sajid. On analytic solution for thin film flow of a fourth grade fluid down a vertical cylinder. *Physics Letters A*, 361(45):316 – 322, 2007.